

GENERATIVE HYPERGRAPH CLUSTERING: FROM BLOCKMODELS TO MODULARITY

Philip S. Chodrow, Nate Veldt, and Austin R. Benson

December 23, 2024

Hypergraphs are a natural modeling paradigm for a wide range of complex relational systems, with components modeled by nodes and interactions between sets of components by hyperedges. A standard analysis task is to identify system modules, corresponding to clusters of closely related or densely interconnected nodes. In the special case of graphs, in which edges connect exactly two nodes at a time, there are a number of probabilistic generative models and associated inference algorithms for clustering; many of these are based on variants of the stochastic blockmodel, a random graph with flexible cluster structure. However, there are few models and algorithms for hypergraph clustering. Here, we propose a Poisson degree-corrected hypergraph stochastic blockmodel (DCHSBM), an expressive generative model of clustered hypergraphs with heterogeneous node degrees and edge sizes. Approximate maximum-likelihood inference in the DCHSBM naturally leads to a clustering objective that generalizes the popular modularity objective for graphs. We derive a general Louvain-type algorithm for this objective, as well as a faster, specialized “All-Or-Nothing” (AON) variant in which edges are expected to lie fully within clusters. This special case encompasses a recent proposal for modularity in hypergraphs, while also incorporating flexible resolution and edge-size parameters. We show that hypergraph Louvain is highly scalable, including as an example an experiment on a synthetic hypergraph of one million nodes. We also demonstrate through synthetic experiments that the detectability regimes for hypergraph community detection differ from methods based on dyadic graph projections. In particular, there are regimes in which hypergraph methods can recover planted partitions even though graph based methods necessarily fail due to information-theoretic limits. We use our model to analyze different patterns of higher-order structure in school contact networks, U.S. congressional bill cosponsorship, U.S. congressional committees, product categories in co-purchasing behavior, and hotel locations from web browsing sessions, finding interpretable higher-order structure. We then study the behavior of our AON hypergraph Louvain algorithm, finding that it is able to recover ground truth clusters in empirical data sets exhibiting the corresponding higher-order structure.

1 INTRODUCTION

Graphs are a fundamental abstraction for complex relational systems throughout the sciences [Jackson, 2008; Easley and Kleinberg, 2010; Newman, 2010]. A graph represents components of a system by a set of nodes, and interactions or relationships among these components using edges that connect pairs of nodes. Much of the structure in complex data, however, involves *higher-order* interactions and relationships between more than two entities at once [Milo, 2002; Benson et al., 2016, 2018; Lambiotte et al., 2019; Battiston et al., 2020; Torres et al., 2020]. People communicate and collaborate in large or small groups. Consumers often purchase multiple items in shopping trips. Chemical interactions occur between sets of molecules of varying size. *Hypergraphs* are now a burgeoning paradigm for modeling these and many other systems [Li and Milenkovic, 2018; de Arruda et al., 2020; Sahasrabuddhe et al., 2020; Veldt et al., 2020b]. A hypergraph

Philip S. Chodrow
 Department of Mathematics
 University of California, Los Angeles
 phil@math.ucla.edu
 Nate Veldt
 Center for Applied Mathematics
 Cornell University
 ntv22@cornell.edu
 Austin Benson
 Department of Computer Science
 Cornell University
 arb@cs.cornell.edu

still represents the components by a set of nodes, but the edges (often called *hyperedges*) may connect arbitrary numbers of nodes. A graph is a special case of a hypergraph, in which each edge connects exactly two nodes.

Given a large complex system, a common analytical task is to break down the system into a relatively small number of *modules* which efficiently summarize the system’s structure [Porter et al., 2009; Benson et al., 2016; Fortunato and Hric, 2016; Li and Milenkovic, 2018]. This task goes under a wide variety of names, such as *clustering*, *partitioning*, *community detection*, and *node classification*. In each case, the high-level goal is to assign each node in the graph or hypergraph to one of a few discrete modules (*clusters*, *sets*, *communities*, *classes*, etc.) such that nodes in the same module are more closely related by the system structure than nodes in differing modules. Because many systems are well-represented by hypergraphs, the problem of identifying modules in hypergraph data has a wide range of applications. In computer science and engineering, hypergraph partitioning has been used to map computations to parallel computers in order to minimize communication costs [Ballard et al., 2016; Kabiljo et al., 2017], optimize circuit layouts [Karypis et al., 1999], and segment images [Agarwal et al., 2005]. Within machine learning and data science, hypergraph clustering and node prediction are used for semi-supervised learning [Zhou et al., 2006; Yadati et al., 2019] and variants of correlation clustering [Li et al., 2019; Amburg et al., 2020; Veldt et al., 2020c]. In network science, hypergraph clustering and community detection have been used to analyze gene expressions [Tian et al., 2009], food webs [Li and Milenkovic, 2017], and online social networks [Neubauer and Obermayer, 2009; Tsourakakis et al., 2017]. For the remainder of this paper, we will usually refer to hypergraph *clustering*, keeping in mind the diversity of approaches and applications falling under this heading.

A key idea for data clustering is to postulate a *probabilistic generative model*. This is a probability distribution over counterfactual realizations of the data, whose unseen parameters include cluster labels for each observation. The problem of assigning nodes to clusters may then be recast as a statistical inference problem. In the context of graph clustering, the most common of these is the stochastic blockmodel (SBM), its variants, and other latent space models [Hoff et al., 2002; Airoldi et al., 2008; Karrer and Newman, 2011; Yang and Leskovec, 2013; Peixoto, 2014; Athreya et al., 2017]. In the standard SBM, each node belongs to an unobserved cluster, or “block”. The probability of an edge existing between two nodes depends only on the block labels of each [Nowicki and Snijders, 2001; Karrer and Newman, 2011]. In the influential planted partition model [Jerrum and Sorkin, 1998; Condon and Karp, 2001], for example, nodes in the same block connect at higher rates than nodes in distinct blocks. In practice, we typically have access to neither the block labels nor the connection rates, and inference techniques are necessary to estimate each.

While generative modeling is a well-developed mainstay of graph clustering approaches, generative techniques for hypergraph clustering are largely lacking. Indeed, while a small number of generative hypergraph models have been proposed [Ghoshdastidar and Dukkipati, 2014; Kim et al., 2018], these models typically generate hypergraphs with edges of only one size. With one recent exception [Ke et al., 2019], these models also do not model degree heterogeneity between nodes. Heterogeneity in edge size and node degree are key features of empirical data [Benson et al., 2018] that we aim to capture. An alternative to modeling hypergraph data directly is to transform the hypergraph to a dyadic graph. This is most commonly done by clique expansion, where a dyadic edge connects any pair of nodes that appear together in some hyperedge [Zhou et al., 2006; Benson et al., 2016]. While this enables the use of a wide array of existing models and algorithms for graphs, the higher-order structure that we want to capture is lost [Chodrow, 2020a], and generative models of the resulting dyadic graph that do not take into account the clique projection may rely on explicitly

violated independence assumptions.

Here we propose a direct generative approach to hypergraph clustering, based on a model of clustered hypergraphs with heterogeneous degree distributions and hyperedge sizes. Our proposed model generalizes the popular degree-corrected stochastic blockmodel (DCSBM) [Karrer and Newman, 2011], and is also related to a recent model for hypergraphs with uniform edge sizes and heterogeneous degrees [Ke et al., 2019]. In our degree-corrected hypergraph stochastic blockmodel (DCHSBM), each node belongs to a latent cluster. The probability of a hyperedge appearing among a given set of nodes depends on the size of the set, the expected degrees of the nodes, and an *affinity function* Ω which governs rates of connections between nodes based on their clusters. We outline a practical approximate coordinate-ascent maximum-likelihood estimation scheme for fitting this model to hypergraph data. This scheme alternates between two steps. In the first, we estimate latent parameters governing node degrees and affinities between cluster labels. This step can be performed in closed form, using a single pass over the data. The second step involves a more difficult (in fact, NP-hard [Brandes et al., 2007]) combinatorial optimization problem. We show that this problem directly generalizes the well-studied modularity objective for graphs. Additionally, when Ω has “All-Or-Nothing” (AON) structure, the resulting modularity objective encompasses recently proposed notion of hypergraph modularity [Kamiński et al., 2019] as an important special case. Our derivation additionally shows how to obtain resolution parameters from the cluster affinity function, which significantly enhances the applicability of this modularity objective to empirical data. For instance, these parameters can be used to down-weight the role of large hyperedges in cases (such as email) in which large interactions may provide weak or no evidence of cluster co-membership. Our alternating framework means that these parameters need not be set by the researcher *a priori*—they can be inferred from data.

In order to perform the second step, we propose an optimization heuristic that generalizes the broadly used Louvain algorithm for modularity maximization in graphs [Blondel et al., 2008]. This algorithm can be used whenever the affinity function possesses symmetric structure. The considerable flexibility in specifying symmetric affinity functions connects our objective function to modeling ideas used for hypergraph partitioning and multiway cut problems [Veldt et al., 2020a]. While the general form of this algorithm is computationally intensive, we derive a specialized algorithm for the AON affinity function that scales well to very large hypergraphs. We conduct synthetic experiments on hypergraphs of size ranging from one thousand to one million nodes, finding that runtime is comparable to fast dyadic methods. In another synthetic experiment, we study the ability of hypergraph AON Louvain to recover planted clusters. We show that hypergraph modularity methods can recover planted clusters in some regimes in which dyadic methods must necessarily fail due to known information-theoretic bounds. This experiment suggests that the theory of detectability in hypergraphs may be substantially more complex than the already-rich theory of detectability in graphs [Abbe, 2017].

We then study a range of empirical systems, including school contact networks, U.S. congressional bill cosponsorships, U.S. congressional committee memberships, co-purchasing, and online hotel browsing. In several of these experiments, our fast alternating modularity maximization scheme is able to find clusters substantially more correlated with supplied data labels than standard approaches based on dyadic modularity. In others experiments, dyadic methods appear weakly preferable. We show how our generative framework enables us to interpret these differing results: the data sets on which our fast algorithm performs well are the data sets in which the corresponding generative model is favored under a penalized likelihood criterion. These results highlight the importance of making explicit the assumptions of clustering algorithms, and matching these assumptions appropriately to data.

2 RELATED WORK

2.1 HYPERGRAPH PARTITIONING AND SPECTRAL CLUSTERING

The need to separate nodes of a hypergraph into various clusters or communities arises in many settings. Applications in VSLI design and scientific computing typically require clusters that are roughly balanced in size; common tools for this task include multilevel partitioning methods such as hMetis [Karypis et al., 1999; Karypis and Kumar, 2000] and KyHyPar [Schlag et al., 2016; Akhremtsev et al., 2017]. Various hypergraph generalizations of spectral graph clustering [Chung, 1992] have been considered in the machine learning and theoretical computer science literature. These perform clustering based on the eigenvectors of some notion of a hypergraph Laplacian. Numerous hypergraph generalizations of the graph Laplacian have been considered, including Laplacians based on graph projections [Bolla, 1993; Li and Solé, 1996; Agarwal et al., 2006; Zhou et al., 2006; Benson et al., 2016; Li and Milenkovic, 2017; Rodríguez, 2003], Laplacian tensors [Chen et al., 2017; Chang et al., 2020], and non-linear Laplacian and p -Laplacian operators [Louis, 2015; Chan et al., 2018; Yoshida, 2019; Li and Milenkovic, 2018]. Other tensor methods for hypergraph community detection have also been developed [Ke et al., 2019]. Although a number of techniques have been already been considered, many of these methods either (i) focus on finding only a single cluster at a time, (ii) are viewed mainly as theoretical results and do not scale well to large data sets or (iii) apply only to k -uniform hypergraphs. There remains a need for theoretically grounded global hypergraph clustering techniques that directly optimize a multicluster objective and scale to large data sets.

2.2 GENERATIVE MODELS FOR HYPERGRAPH CLUSTERING

There exist several generative models for hypergraphs with cluster or community structure. The simplest of these is the k -uniform hypergraph stochastic blockmodel, or k -HSBM [Ghoshdastidar and Dukkipati, 2014]. In a k -uniform hypergraph, all edges consist of exactly k nodes. In the k -HSBM, for each k -tuple of nodes, the probability of realizing an edge on those nodes is a function only of the community labels of those nodes. When this function is chosen to favor sets of nodes with identical labels, cluster structure emerges. The k -HSBM is an important testbed for studying the theoretical limitations of hypergraph partitioning algorithms [Kim et al., 2018]. It is, however, limited in its applicability to empirical hypergraph data sets, which are not usually uniform. Additionally, the k -HSBM tends to generate hypergraphs in which the degrees of nodes within the same cluster are tightly concentrated, contrasting to many real-world networks in which degrees are highly heterogeneous. A recent proposal by Ke et al. [2019] generates degree-heterogeneous hypergraphs and is closely related to our proposal below, but the authors do not directly use the statistical structure of their model in their accompanying algorithm.

Another generative approach to hypergraph clustering uses the correspondence between hypergraphs and bipartite graphs. To construct the bipartite graph B from a hypergraph H , we associate to each node i a bipartite node u_i and to each edge e a bipartite node v_e . An edge (u_i, v_e) exists in the bipartite graph B if and only if $i \in e$ (in H). Larremore et al. [2014] developed a degree-corrected stochastic blockmodel for bipartite networks (biSBM), which has since been extended via Bayesian tools [Yen and Larremore, 2020]. In principle, one can use these models to perform inference in hypergraphs. One first obtains the bipartite graph B , constructs an estimate or posterior distribution over nodes $\{u_i\}$, and then returns this estimate. This approach, however, involves statistical assumptions which require examination. Bipartite edges in the biSBM are conditionally independent given the model parameters. As a result, the biSBM is unable to model higher-order dependence in edges, such as the “All-Or-Nothing” dependence which we

discuss later. Bipartite methods may still be appropriate for certain hypergraph data sets, but, like any statistical model, their assumptions must be appropriately matched to data. There is considerable value in the presence of multiple generative models with clear statements of their statistical assumptions.

2.3 MODULARITY METHODS FOR GRAPHS AND HYPERGRAPHS

Modularity maximization is a popular heuristic for clustering dyadic graphs. In the original development [Newman and Girvan, 2004], the authors define a *modularity objective* Q . Let \mathbf{A} be the (possibly weighted) adjacency matrix of an undirected graph, with a_{ij} being the number or total weight of edges linking nodes i and j . Let $\mathbf{d} = \mathbf{A}\mathbf{e}$ be the vector of node degrees, where \mathbf{e} is the vector of ones. Then, $m = \frac{1}{2}\mathbf{e}^T\mathbf{A}\mathbf{e}$ gives the total edge weight in the graph. Finally, let $\mathbf{z} \in [\bar{\ell}]^n$ be the vector of node labels, where $\bar{\ell}$ is the number of distinct clusters. The modularity Q is then defined as

$$Q(\mathbf{z}) \equiv \frac{1}{m} \sum_{i < j} \left[a_{ij} - \frac{d_i d_j}{2m} \right] \delta(z_i, z_j). \quad (1)$$

The modularity $Q(\mathbf{z})$ is thus a sum of differences between the observed number of edges a_{ij} and the term $\frac{d_i d_j}{2m}$, with the (i, j) th term only appearing if $z_i = z_j$.¹ The term $\frac{d_i d_j}{2m}$ is intended to reflect the expected number of edges between i and j under a configuration-type null model, although the question of precisely which model is applied is often obscure in the literature [Chodrow, 2020b]. Subsequent developments [Reichardt and Bornholdt, 2006; Fortunato and Barthélémy, 2007] incorporated a *resolution parameter* γ premultiplying the second term, which can be systematically varied in order to gain insight into community structure at multiple scales [Weir et al., 2017]. There is considerable latitude to make more dramatic alterations to the second term, such as accounting for spatial correlations in social networks [Expert et al., 2011] or applying alternative null distributions over graphs [Fosdick et al., 2018; Chodrow, 2020b].

Theoretically, the modularity objective can be understood from either dynamical [Delvenne et al., 2010] or statistical [Zhang and Moore, 2014; Newman, 2016] perspectives. In practice, the popularity of modularity maximization reflects the existence of highly scalable heuristics, of which the most popular is the Louvain algorithm [Blondel et al., 2008] and variants [Traag et al., 2019]. Modularity maximization, however, possesses a number of important limitations. First, it is an NP-hard problem [Brandes et al., 2007]. Any given output partition of a heuristic is therefore not guaranteed to be the true global maximum of (1). There are often many uncorrelated partitions with nearly optimal modularity scores, complicating the interpretation of any single partition [Good et al., 2010]. Modularity maximization, like all community-detection methodologies, must also grapple with the fact that in many empirical networks, ground truth partitions may be only weakly correlated—or entirely uncorrelated—with network structure [Peel et al., 2017].

Despite these limitations, modularity maximization remains an important method for graph clustering. A natural question is how to extend modularity maximization to the setting of hypergraphs. One method is to apply the dyadic objective (1) to a dyadic graph G derived from a hypergraph H . One forms the clique-expansion graph G , in which each hyperedge in H is represented by a clique in G , and then applies (1) or one of its variants. Such a direct approach effectively discards the polyadic structure in the original data, and can also lead to a combinatorial explosion of dyadic edges when the hyperedges have many nodes. An alternative which does preserve some higher-order information is again to use the correspondence between hypergraphs and bipartite graphs. There are several extant proposals for bipartite modularities [Barber, 2007; Guimerà et al., 2007; Murata, 2009b,a; Liu and Murata, 2010]. To our knowledge, the limitations and implicit statistical assumptions of these modularities remain relatively unexplored.

¹ Throughout this paper, we use the notation that $\delta(a, b) = 1$ if the arguments a and b are the same and $\delta(a, b) = 0$ otherwise.

It is also possible to define modularity objectives directly on hypergraphs. Kumar et al. [2020] consider an approach that alternates between Louvain on a weighted clique-expansion graph G and re-weighting of the graph edges according to a polyadic cut penalty. Kamiński et al. [2019] instead define a modularity objective by comparing the observed hypergraph to the expectation of a generalized Chung-Lu model [Chung and Lu, 2002] for hypergraphs. They derive a modularity objective of the form

$$Q(\mathbf{z}) = \sum_{\ell=1}^{\bar{\ell}} \left[E_\ell - \sum_{k \geq 2}^{\bar{k}} m_k \left(\frac{\mathbf{vol}(\ell)}{\mathbf{vol}(H)} \right)^k \right], \quad (2)$$

where $\bar{\ell}$ is the number of clusters, E_ℓ is the number of hyperedges that fall fully within cluster ℓ , m_k is the number of hyperedges of size k , $\mathbf{vol}(\ell) = \sum_{i=1}^n d_i \delta(z_i, \ell)$ is the sum of degrees within cluster i , and $\mathbf{vol}(H) = \sum_{i=1}^n d_i$ is the sum of degrees within the entire hypergraph. They also propose a stagewise greedy algorithm based on that of Clauset et al. [2004] for heuristically optimizing this objective. We will later generalize (2) via our generative model.

3 THE DEGREE-CORRECTED HYPERGRAPH STOCHASTIC BLOCKMODEL

The degree-corrected stochastic blockmodel is a generative model of graphs with both community structure and heterogeneous degree sequences [Karrer and Newman, 2011]. We now extend this model to the case of hypergraphs.

First, we introduce some notation. Fix a number of nodes $n \in \mathbb{Z}_+$, and let $\mathcal{N} = [n]$ be a set of nodes.² For each $k \in \mathbb{Z}_+$, let $\mathcal{T}_k \equiv \mathcal{N}^k$, and let $\mathcal{T} \equiv \bigcup_{k=1}^{\bar{k}} \mathcal{T}_k$ so that \mathcal{T} is the set of ordered tuples of nodes of length no longer than \bar{k} . By definition, the same node may appear in an element of \mathcal{T} multiple times; this choice is traditional in the stochastic blockmodel literature and significantly simplifies certain calculations below. It is notationally convenient, however, for sums to range over the set \mathcal{R} of *unordered* node tuples. Write $R \sim T$ if tuples R and T differ only by a permutation of their elements. Each element R of \mathcal{R} corresponds to b_R elements of \mathcal{T} , where b_R is the number of distinct ways to order the elements of R . If $|R| = k$, then $b_R = \binom{k}{k_1(R), \dots, k_n(R)}$, where $k_i(R)$ is the number of times that node i appears in R . We regard each element of \mathcal{R} as the location of a possible edge in a hypergraph H . For any vector $\mathbf{v} \in \mathbb{R}^n$ and $T = (t_1, \dots, t_k) \in \mathcal{T}$, we define $\mathbf{v}_T \equiv (v_{t_1}, \dots, v_{t_k})$. Let \mathbf{v}_R for $R \in \mathcal{R}$ be defined similarly. Next, let $\sigma(\mathbf{v}) \equiv \prod_{i=1}^n v_i$ for any vector $v \in \mathbb{R}^m$. Finally, we let $a_R \in \mathbb{Z}_{\geq 0}$ be the number of hyperedges on the nodes specified by R .

We now parameterize our model. As in the dyadic degree-corrected SBM, we assign to each node i a parameter θ_i which governs its degree. These parameters are collected in a vector $\boldsymbol{\theta} \in \mathbb{R}^n$. To each node i we assign one of $\bar{\ell}$ groups $z_i \in [\bar{\ell}]$, and collect these assignments in a vector $\mathbf{z} \in [\bar{\ell}]^n$. In our notation, \mathbf{z}_R and \mathbf{z}_T give the labels of the nodes in R (unordered) or T (ordered). Let Ω be an *affinity function* which maps unordered tuples of node labels to nonnegative real numbers. If $\Omega(\mathbf{z}_R)$ is large, this implies that nodes in the group configuration \mathbf{z}_R connect at a relatively high rate. For convenience, we will also say that $\Omega(\mathbf{z}_T) = \Omega(\mathbf{z}_R)$ when $R \sim T$. We allow Ω to remain fully general at this stage.

For fixed \mathbf{z} , $\boldsymbol{\theta}$, and Ω , we generate a hypergraph by sampling, for each $T \in \mathcal{T}$,

$$a_T \sim \text{Poisson}(\sigma(\boldsymbol{\theta}_T) \Omega(\mathbf{z}_T))$$

and then setting

$$a_R = \sum_{T: R \sim T} a_T.$$

² Here and elsewhere, we use the notation $[r] = \{1, \dots, r\}$.

Here, R , which is unordered, is a possible location for a weighted hyperedge, and it is realized by repeated attempts to “lay down” ordered tuples T onto R , for all $T \sim R$. The value of a_R can be any positive integer, representing multiple hyperedges on R . This is a helpful modeling feature, as many empirical hypergraphs indeed contain multiple hyperedges between the same set of nodes.³ The probability of realizing a given edge set \mathcal{A} is the product of probabilities over the individual entries:

$$\mathbb{P}(\mathcal{A}|\mathbf{z}, \Omega, \boldsymbol{\theta}) = \prod_{R \in \mathcal{R}} \mathbb{P}(a_R|\mathbf{z}, \Omega) = \prod_{R \in \mathcal{R}} \frac{e^{-b_R \sigma(\boldsymbol{\theta}_R) \Omega(\mathbf{z}_R)} (b_R \sigma(\boldsymbol{\theta}_R) \Omega(\mathbf{z}_R))^{a_R}}{a_R!}.$$

We have used the fact that $a_R = \sum_{T:R \sim T} a_T$ is a sum of b_R i.i.d. Poisson random variables with parameter $\sigma(\boldsymbol{\theta}_T) \Omega(\mathbf{z}_T) = \sigma(\boldsymbol{\theta}_R) \Omega(\mathbf{z}_R)$, and is therefore itself Poisson with parameter $b_R \sigma(\boldsymbol{\theta}_R) \Omega(\mathbf{z}_R)$.

3.1 ESTIMATION OF DEGREE AND AFFINITY PARAMETERS

There are many methods for inference in stochastic blockmodels and their relatives, including variational coordinate ascent [Airoldi et al., 2008], variational belief propagation [Decelle et al., 2011; Zhang and Moore, 2014], and Markov Chain Monte Carlo [Peixoto, 2019]. We use maximum-likelihood inference, a highly simplified approach. We do so in order to exploit a recent connection between maximum-likelihood inference in stochastic blockmodels and the popular modularity objective for graph clustering [Newman, 2016].

In the maximum-likelihood framework, we learn estimates $\hat{\mathbf{z}}$ of the node labels, $\hat{\Omega}$ of the affinity function, and $\hat{\boldsymbol{\theta}}$ of the degree parameters by solving the optimization problem

$$\hat{\mathbf{z}}, \hat{\Omega}, \hat{\boldsymbol{\theta}} \equiv \underset{\mathbf{z}, \Omega, \boldsymbol{\theta}}{\operatorname{argmax}} \mathbb{P}(\mathbf{A}|\mathbf{z}, \Omega, \boldsymbol{\theta}), \quad (3)$$

where \mathbf{A} is a given data set represented by a collection of (integer-weighted) hyperedges. As usual, it is easier to work with the log-likelihood, which has the same local optima. The log-likelihood is

$$\mathcal{L}(\mathbf{z}, \Omega, \boldsymbol{\theta}) = \sum_{R \in \mathcal{R}} \log \mathbb{P}(a_R|\mathbf{z}, \Omega, \boldsymbol{\theta}) = Q(\mathbf{z}, \Omega, \boldsymbol{\theta}) + K(\boldsymbol{\theta}) + C, \quad (4)$$

where

$$\begin{aligned} Q(\mathbf{z}, \Omega, \boldsymbol{\theta}) &\equiv \sum_{R \in \mathcal{R}} [a_R \log \Omega(\mathbf{z}_R) - b_R \sigma(\boldsymbol{\theta}_R) \Omega(\mathbf{z}_R)] \\ K(\boldsymbol{\theta}) &\equiv \sum_{R \in \mathcal{R}} a_R \log \sigma(\boldsymbol{\theta}_R) \\ C &\equiv \sum_{R \in \mathcal{R}} [a_R \log b_R - \log a_R!] . \end{aligned}$$

The first term $Q(\mathbf{z}, \Omega, \boldsymbol{\theta})$ is the only part of the log-likelihood that depends on the group assignments \mathbf{z} and affinity function Ω . The second term depends on $\boldsymbol{\theta}$, while the third term depends only on the data \mathbf{A} and can be disregarded for inferential purposes.

When solving (3), there are two forms of statistical unidentifiability that prevent us from learning unique estimates. First, permuting the group labels in \mathbf{z} and Ω does not alter \mathcal{L} . Thus, we impose an arbitrary order on group labels. Another form of unidentifiability is slightly more subtle. Fix $\boldsymbol{\theta}$ and Ω . Fix $\ell \in [\bar{\ell}]$ and $s \in \mathbb{R}$. We construct a modified vector $\boldsymbol{\theta}'$ given by

$$\theta'_i = \begin{cases} s\theta_i & z_i = \ell \\ \theta_i & \text{otherwise.} \end{cases}$$

³ Even in hypergraph data sets where we only know the presence or absence of hyperedges (but no weights), the Poisson-based model serves as a computationally convenient approximation to a Bernoulli-based model.

Define the modified affinity function $\Omega'(\mathbf{z}_R) = s^{-k_\ell(\mathbf{z}_R)}\Omega(\mathbf{z}_R)$, where $k_\ell(\mathbf{z}_R)$ is the number of times that label ℓ appears in \mathbf{z}_R . By construction, $\mathcal{L}(\mathbf{z}, \Omega, \boldsymbol{\theta}) = \mathcal{L}(\mathbf{z}, \Omega', \boldsymbol{\theta}')$. To enforce identifiability, we must therefore place a joint normalization condition on $\boldsymbol{\theta}$ and Ω . We do so by enforcing

$$\sum_{i=1}^n \theta_i \delta(z_i, \ell) = \mathbf{vol}(\ell), \quad \ell = 1, \dots, \bar{\ell}, \quad (5)$$

where $\mathbf{vol}(\ell) = \sum_{i=1}^n d_i \delta(z_i, \ell)$ and d_i is the (weighted) number of hyperedges in which node i appears, i.e. $d_i = \sum_{R \in \mathcal{R}: i \in R} a_R$. The utility of (5) is that, when \mathbf{z} is known or estimated, the estimates $\hat{\boldsymbol{\theta}}$ and $\hat{\Omega}$ take simple, closed forms, as we show next. Later, in Section 4, we provide algorithms for estimating \mathbf{z} .

Using (5), it is possible to show that

$$\sum_{R \in \mathcal{R}} b_R \sigma(\boldsymbol{\theta}_R) \Omega(\mathbf{z}_R) = \sum_{k=1}^{\bar{k}} \sum_{\mathbf{y} \in [\bar{\ell}]^k} \Omega(\mathbf{y}) \prod_{y \in \mathbf{y}} \mathbf{vol}(y). \quad (6)$$

A proof is given in Appendix A. This identity implies that the second term of Q does not depend on $\boldsymbol{\theta}$ once the normalization (5) has been enforced. Since the first term of Q is also independent of $\boldsymbol{\theta}$, we can compute the estimate $\hat{\boldsymbol{\theta}}$ by maximizing $K(\boldsymbol{\theta})$ alone. We write

$$K(\boldsymbol{\theta}) = \sum_{R \in \mathcal{R}} a_R \log \sigma(\boldsymbol{\theta}_R) = \sum_{R \in \mathcal{R}} a_R \sum_{j \in R} \log \theta_j. \quad (7)$$

The first-order optimality conditions on $\boldsymbol{\theta}$ from the objective (7) with constraint (5) imply that $K(\boldsymbol{\theta})$ is maximized with respect to θ_i when $\hat{\theta}_i = \sum_{R \in \mathcal{R}} k_i(R) a_R = d_i$. The maximum-likelihood estimate is thus $\hat{\boldsymbol{\theta}} = \mathbf{d}$. Notably, though our derivation assumed that \mathbf{z} was fixed, it is not necessary to *know* \mathbf{z} in order to form the estimate $\hat{\boldsymbol{\theta}}$.

We now consider the estimation of Ω . We focus on the case in which Ω takes constant value ω on some set Y of unordered tuples of labels.⁴ Inserting (6) into the definition of Q and differentiating with respect to ω yields, as consequence of the first-order optimality condition, the closed-form estimate

$$\hat{\omega} = \frac{\sum_{\mathbf{y} \in Y} \sum_{R \in \mathcal{R}} a_R \delta(\mathbf{z}_R, \mathbf{y})}{\sum_{\mathbf{y} \in Y} \prod_{y \in \mathbf{y}} \mathbf{vol}(y)}. \quad (8)$$

Algebraic details are supplied in Appendix B. In contrast to the maximum-likelihood estimate $\boldsymbol{\theta} = \mathbf{d}$, the estimate $\hat{\omega}$ requires that we know or estimate \mathbf{z} . We turn to this problem next.

4 HYPERGRAPH MODULARITIES

Our results from the previous section imply that the estimated degree parameter $\hat{\boldsymbol{\theta}}$ and piecewise constant affinity function $\hat{\Omega}$ can be efficiently estimated in closed form, provided an estimate of \mathbf{z} . This naturally suggests a coordinate-ascent optimization scheme, in which we alternate between estimating these parameters and estimating \mathbf{z} . We now discuss the latter step. From (4), it suffices to optimize Q with respect to \mathbf{z} . To do so, it is helpful to impose some additional structure on $\hat{\Omega}$.

4.1 SYMMETRIC MODULARITIES

We obtain an important class of objective functions by stipulating that Ω is symmetric with respect to permutations of node labels. In this case, $\Omega(\mathbf{z}_R)$ depends not on the specific labels in \mathbf{z}_R , but only on the number of repetitions of

⁴In full generality, we can have one such ω for every possible label arrangement for each hyperedge size in the data. Later, we will make natural restrictions on Ω .

each. Statistically, the corresponding DCHSBM generates hypergraphs in which all groups are statistically identical, conditioned on the degrees of their constituent nodes. Symmetric affinity functions thus lead to a flexible generalization of the planted partition stochastic blockmodel [Jerrum and Sorkin, 1998; Condon and Karp, 2001] to the setting of hypergraphs.

Define the function $\phi(\mathbf{z}) = \mathbf{p}$, where p_j is the number of entries of \mathbf{z} in the j th largest group in \mathbf{z} , with ties broken arbitrarily. For example, if $\mathbf{z} = (1, 1, 1, 2, 2, 3, 4)$, then $\mathbf{p} = (3, 2, 1, 1)$. We call \mathbf{p} a *partition vector*. The symmetry assumption implies that Ω is a function of \mathbf{z}_R only through $\mathbf{p} = \phi(\mathbf{z}_R)$. Accordingly, we abuse notation by writing $\Omega(\mathbf{p}) \equiv \Omega(\mathbf{z})$ when $\mathbf{p} = \phi(\mathbf{z})$.

It is convenient to now define generalized cuts and volumes corresponding to the partition vector \mathbf{p} . Fix $k = \mathbf{e}^T \mathbf{p}$, the number of elements in a label vector with partition \mathbf{p} . Then we define

$$\begin{aligned}\mathbf{cut}_{\mathbf{p}}(\mathbf{z}) &\equiv \sum_{R \in \mathcal{R}^k} a_R \delta(\mathbf{p}, \phi(\mathbf{z}_R)), \\ \mathbf{vol}_{\mathbf{p}}(\mathbf{z}) &\equiv \sum_{\mathbf{y} \in [\bar{\ell}]^k} \delta(\mathbf{p}, \phi(\mathbf{y})) \prod_{y \in \mathbf{y}}^k \mathbf{vol}(y).\end{aligned}$$

The function $\mathbf{cut}_{\mathbf{p}}(\mathbf{z})$ counts the number of edges that are split by \mathbf{z} into the partition \mathbf{p} , while the function $\mathbf{vol}_{\mathbf{p}}(\mathbf{z})$ is a sum-product of volumes over all grouping vectors \mathbf{y} that induce partition \mathbf{p} . Let \mathcal{P} be the set of partition vectors on sets up to size $\bar{\ell}$. We show in Appendix C that the symmetric modularity objective can then be written as

$$Q(\mathbf{z}, \Omega, \mathbf{d}) = \sum_{\mathbf{p} \in \mathcal{P}} [\mathbf{cut}_{\mathbf{p}}(\mathbf{z}) \log \Omega(\mathbf{p}) - \mathbf{vol}_{\mathbf{p}}(\mathbf{z}) \Omega(\mathbf{p})]. \quad (9)$$

Direct calculation of $\mathbf{vol}_{\mathbf{p}}(\mathbf{z})$ requires the summation of $\bar{\ell}^k$ elements, which can be impractical when either $\bar{\ell}$ or k are large. However, it is possible to evaluate these sums efficiently via a combinatorial identity. Define

$$U_{\mathbf{p}} \equiv \mathbf{vol}_{\mathbf{p}}(\mathbf{z}) \binom{k}{\mathbf{p}}^{-1} \prod_{j=1}^k |\{h : p_h = j\}|!.$$

The number $U_{\mathbf{p}}$ is an order-corrected version of the moments $\mathbf{vol}_{\mathbf{p}}(\mathbf{z})$ in which there is a single term for each distinct partition vector \mathbf{p} . Let \mathbf{e}_j be the j th standard basis vector. For each k , let $\mu_k = \sum_{\ell=1}^{\bar{\ell}} \mathbf{vol}(\ell)^k$; these moments can be computed in $O(nk)$ time.

Proposition 1. *Fix \mathbf{p} , and let $r = \|\mathbf{p}\|_0$ be the number of nonzero elements of \mathbf{p} . Then,*

$$U_{\mathbf{p}} = \mu_{p_r} U_{\mathbf{p} - p_r \mathbf{e}_r} - \sum_{j=1}^{r-1} U_{\mathbf{p} + p_r (\mathbf{e}_j - \mathbf{e}_r)}.$$

A proof is given in Appendix E. We also give a formula for updating the entire set of moments $\{U_{\mathbf{p}}\}$ when a candidate labeling \mathbf{z} is modified.

The objective function (9) is related in approach to the multiway hypergraph cut problem studied by Veldt et al. [2020a]. They formulate the hypergraph cut objective in terms of *splitting functions*, which associate penalties when edges are split between two or more clusters. One then aims to minimize the sum of penalties subject to constraints that certain nodes must not lie in the same cluster. Symmetric affinity functions in our framework correspond to *signature-based splitting functions* in their terminology. Table 1 lists four of many families of affinity functions. The All-Or-Nothing affinity function distinguishes only

whether or not a given edge is contained entirely within a single cluster. This affinity function is especially important for scalable computation, and we discuss it further below. The Group Number affinity depends only on the number of distinct groups represented in an edge, regardless of the number of incident nodes in each one. Special cases of the Group Number affinity arise frequently in applications. When $f(\|\mathbf{p}\|_0, k) = \exp(\|\mathbf{p}\|_0 - 1)$, the first term of the modularity objective corresponds to a hyperedge cut penalty that is known in the scientific computing literature as connectivity – 1 [Deveci et al., 2015], the $K - 1$ metric [Karypis and Kumar, 2000], or the boundary cut [Hendrickson and Kolda, 2000]. It has also been called *fanout* in the database literature [Kabiljo et al., 2017]. The related Sum of External Degrees penalty [Karypis and Kumar, 2000] is also a special case of the Group Number affinity. The Relative Plurality affinity considers only the relative difference between the size of the largest group represented in an edge and the next largest group. This rather specialized affinity function is especially appropriate in contexts where groups are expected to be roughly balanced, as we find, for example, in party affiliations in Congressional committees. Finally, the Pairwise affinity counts the number of pairs of nodes within the edge whose clusters differ. While this affinity function uses similar information to that used in dyadic graph models, there is no immediately apparent equivalence between any dyadic random graph and a DCHSBM with the Pairwise affinity function. There are many more symmetric affinity functions; see Table 3 of Veldt et al. [2020a] for several other splitting functions which can be used to define affinities.

An important subtlety was recently raised by Zhang and Peixoto [2020] concerning the relationship between blockmodels and modularity in Newman [2016], which also applies to our derivation of (9) and (10) below. We derived the maximum-likelihood estimates of θ and Ω under the assumption of a general, unconstrained affinity function Ω . It is not guaranteed that this same estimate maximizes the likelihood when symmetric or other constraints are placed on Ω . Indeed, as Zhang and Peixoto [2020] show, the estimate $\hat{\theta} = \mathbf{d}$ only coincides with exact maximum-likelihood for constrained Ω when $\text{vol}(\ell)$ is constant for each $\ell \in [\hat{\ell}]$. When the sizes of groups vary, as is typical in most data sets, this simple estimate is instead an approximation of the exact maximum-likelihood estimate. The situation is reminiscent of the known tendency of the graph modularity objective to generate clusters of approximately equal sizes [Gleich and Mahoney, 2016]. The objectives and algorithms we develop below should therefore be understood as approximations, which are exact only in the case that all clusters have equal volumes.

All-Or-Nothing (AON)	$\Omega(\mathbf{p}) = \begin{cases} \omega_{k1} & \ \mathbf{p}\ _0 = 1 \\ \omega_{k0} & \text{otherwise.} \end{cases}$
Group Number (GN)	$\Omega(\mathbf{p}) = f(\ \mathbf{p}\ _0, k)$
Relative Plurality (RP)	$\Omega(\mathbf{p}) = g(p_1 - p_2, k)$
Pairwise (P)	$\Omega(\mathbf{p}) = h\left(\sum_{i \neq j} p_i p_j, k\right)$

Table 1 – Symmetric affinity functions. Throughout, $k = \|\mathbf{p}\|_1$ is the number of nodes in partition \mathbf{p} , ω_{k0} and ω_{k1} are scalars, and f , g , and h are arbitrary scalar functions.

4.2 ALL-OR-NOTHING MODULARITY

As noted above, the All-Or-Nothing affinity function (Table 5) is of special interest for modeling and computation. This affinity function is a natural choice for systems in which the occurrence of an interaction or relationship depends strongly on homogeneity within groups.

Inserting the All-Or-Nothing affinity function from Table 1 into (9) yields, after a small amount of algebra, the objective

$$Q(\mathbf{z}, \Omega, \mathbf{d}) = - \sum_{k=1}^{\bar{k}} \beta_k \left[\mathbf{cut}_k(\mathbf{z}) + \gamma_k \sum_{\ell=1}^{\bar{\ell}} \mathbf{vol}(\ell)^k \right] + J(\boldsymbol{\omega}), \quad (10)$$

where $\beta_k = \log \omega_{k1} - \log \omega_{k0}$, $\gamma_k = \beta_k^{-1}(\omega_{k1} - \omega_{k0})$, and $J(\boldsymbol{\omega})$ collects terms that do not depend on the partition \mathbf{z} . We collect $\{\beta_k\}$ and $\{\gamma_k\}$ into vectors $\boldsymbol{\beta}, \boldsymbol{\gamma} \in \mathbb{R}^{\bar{k}}$. Let m_k be the (weighted) number of hyperedges of size k , i.e., $m_k = \sum_{R \in \mathcal{R}_k} a_R$. We have also defined

$$\text{cut}_k(\mathbf{z}) \equiv m_k - \sum_{R \in \mathcal{R}_k} a_R \delta(\mathbf{z}_R)$$

as the number of hyperedges of size k which contain nodes in two or more distinct clusters. This calculation is a direct generalization of that from [Newman \[2016\]](#) for graph modularity. Indeed, we recover the standard dyadic modularity objective by restricting to $k = 2$. We call (10) the *All-Or-Nothing (AON) hypergraph modularity*.

Recently, [Kamiński et al. \[2019\]](#) proposed a “strict modularity” objective for hypergraphs. This strict modularity is a special case of (10), obtained by choosing ω_{k0} and ω_{k1} such that $\beta_k = 1$ and $\gamma_k = \frac{m_k}{(\text{vol}(H))^k}$. However, leaving these parameters free lends important flexibility to our proposed AON objective (10). Tuning β_k allows one to specify which hyperedge sizes are considered to be most relevant for clustering. In email communications, for example, a very large list of recipients may carry minimal information about their social relationships, and it may be desirable to down-weight large hyperedges by tuning $\boldsymbol{\beta}$. Tuning $\boldsymbol{\gamma}$ has the effect of modifying the sizes of clusters favored by the objective, in a direct generalization of the resolution parameter in dyadic modularity [[Reichardt and Bornholdt, 2006](#); [Veldt et al., 2018](#)]. Importantly, it is not necessary to specify the values of these parameters *a priori*; instead, they can be adaptively estimated via (8).

5 HYPERGRAPH MAXIMUM-LIKELIHOOD LOUVAIN

In order to optimize the modularity objectives (9) and (10), we propose a family of agglomerative clustering algorithms. These algorithms greedily improve the specified objective through local updates to the node label vector \mathbf{z} . The structure of these algorithms is based on the widely used and highly performant Louvain heuristic for graphs [[Blondel et al., 2008](#)]. The standard heuristic alternates between two phases. In the first phase, each node begins in its own singleton cluster. Then, each node i is visited and moved to the cluster of the adjacent node j which maximizes the increase in the objective Q . If no such move increases the objective, then i ’s label is not changed. This process repeats until no such moves exist which increase the objective. In the second phase, a “supernode” is formed for each label. The supernode represents the set of all nodes sharing that label. Then, the first phase is repeated, generating an updated labeling of supernodes, which are then aggregated in the second phase. The process repeats until no more improvement is possible. Since every step in the first phase improves the objective, the algorithm terminates with a locally optimal cluster vector \mathbf{z} .

This heuristic generalizes naturally to the setting of hypergraphs. However, the incorporation of heterogeneous hyperedge sizes and general affinity functions considerably complicates implementation. Here we provide a highly general Hypergraph Maximum-Likelihood Louvain (HMLL) algorithm for optimizing the symmetric modularity objective (9). For the important case of the All-Or-Nothing (AON) affinity, the simplified objective (10) admits a much simpler and faster specialized Louvain algorithm, which we describe in [Appendix F](#). As we show in subsequent experiments, this specialized algorithm is highly scalable and effective in recovering ground truth clusters in data sets with polyadic structure plausibly modeled by the AON affinity.

Algorithm 1: SymmetricHMLLstep(H, Ω, \mathbf{z})

Data: Hypergraph H , affinity function Ω , current label vector \mathbf{z}

Result: Updated label vector \mathbf{z}

```
 $\mathcal{C} \leftarrow \text{unique}(\mathbf{z})$  // unique cluster labels in  $\mathbf{z}$ 
 $\mathbf{z}' \leftarrow \mathbf{z}$ 
improving  $\leftarrow$  true
while improving do
  improving  $\leftarrow$  false
  for  $c$  in  $\mathcal{C}$  do
     $S_c \leftarrow \{i: z_i = c\}$  // set of nodes with label  $c$ 
     $\mathcal{A}_c \leftarrow \bigcup_{e \in E} \{c' \in \mathcal{C}: S_c \cap e \neq \emptyset, S_{c'} \cap e \neq \emptyset\}$  // adjacent clusters
    // maximum  $\Delta$  and maximizer  $c'$  of the change in  $Q$  from moving
    // node  $i$  to adjacent cluster  $\tilde{c} \in \mathcal{A}_c$ 
     $(\Delta, c') \leftarrow \text{argmax}_{\tilde{c} \in \mathcal{A}_c} \Delta Q(H, \Omega, \mathbf{z}, S_c, \tilde{c})$ 
    // update  $\mathbf{z}$  if improvement found
    if  $\Delta > 0$  then
      for  $i$  in  $c$  do
         $| z_i \leftarrow c'$ 
      end
      improving  $\leftarrow$  true
    end
  end
end
return  $\mathbf{z}$ 
```

Algorithm 2: SymmetricHMLL(H, Ω)

Data: Hypergraph H , affinity function Ω

Result: Label vector \mathbf{z}

```
 $\mathbf{z}' \leftarrow \mathbf{z} \leftarrow [n]$  // assign each cluster to singleton
do
   $\mathbf{z} \leftarrow \mathbf{z}'$ 
   $\mathbf{z}' \leftarrow \text{SymmetricHMLLstep}(H, \Omega, \mathbf{z})$ 
while  $\mathbf{z} \neq \mathbf{z}'$ 
return  $\mathbf{z}$ 
```

5.1 SYMMETRIC HYPERGRAPH MAXIMUM-LIKELIHOOD LOUVAIN

We first show pseudocode for a single step of Symmetric HMLL in Algorithm 1. In this step, we visit each cluster S_c of nodes sharing a label c , and consider changing the label of all nodes in S_c to c' , where c' is a new label such that at least one edge is incident on both S_c and $S_{c'}$. We evaluate the change ΔQ in the objective function Q associated with this change. We then carry out the change that gives the largest change in objective, provided that change is positive. After visiting each cluster S_c , the process is repeated until no more improvements are possible. This process is repeated in an outer loop given by Algorithm 2. After initializing each node in a singleton cluster, we then alternate between consolidating nodes by their cluster assignments and modifying node labels via Algorithm 1.

Algorithm 1 relies on a function ΔQ which computes the change in the objective Q associated with moving all nodes in cluster c to cluster c' . Changes to the second (volume) term in the objective can be computed efficiently using Proposition 1. Evaluating changes to the first (cut) term requires summing across all hyperedges incident to a node or set of nodes. At each hyperedge, we must evaluate the affinity $\Omega(\mathbf{p})$ on the current partition \mathbf{p} , as well as the affinity $\Omega(\mathbf{p}')$

associated with the candidate updated partition \mathbf{p}' . This situation contrasts with the case of the dyadic graph Louvain algorithm, in which it is sufficient to simply check whether a given edge joins nodes in the same or different clusters. Because we need to store and update the partition vector \mathbf{p} for each hyperedge, we cannot collapse clusters of nodes into monolithic supernodes and recursively apply Algorithm 2 on a reduced data structure, as customary in dyadic graph Louvain. Thus, while clusters of nodes move as a unit in Algorithm 1 as well, it is necessary in this case to operate on the full adjacency data \mathcal{A} at all stages of the algorithm. This implies that Algorithm 2 can be slow on hypergraphs of even modest size. The development of efficient algorithms for optimizing the general symmetric modularity objective or various special cases is an important avenue of future work.

5.2 ALL-OR-NOTHING HYPERGRAPH MAXIMUM-LIKELIHOOD LOUVAIN

When Ω is the All-Or-Nothing affinity function, considerable simplification is possible. For each edge we need not compute the full partition vector \mathbf{p} but only check whether or not $\|\mathbf{p}\|_0 = 1$. Rather than a general affinity function Ω , we instead supply the parameter vectors β and γ appearing in (10). This allows us to compute on considerably simplified data structures. In particular, we are able to follow the classical Louvain strategy of collapsing clusters into single, consolidated “supernodes,” and restrict attention to hyperedges that span multiple supernodes. Because we do not need to track the precise *way* in which the hyperedges span multiple supernodes, we can forget much of the original adjacency data \mathcal{A} and instead simply store the edge sizes of the hypergraph. These simplifications enable both significant memory savings and very rapid evaluation of the objective update function ΔQ . We provide pseudocode for exploiting these simplifications in Appendix F.

6 EXPERIMENTS WITH SYNTHETIC DATA

6.1 RUNTIME

Dyadic Louvain algorithms are known for being highly efficient in large graphs. Here, we show that AON HMLL can achieve similar performance on synthetic data to Graph MLL (GMLL), a variant of the standard dyadic Louvain algorithm in which we return the combination of resolution parameter and partition that yield the highest dyadic likelihood. For a fixed number of nodes n , we consider a DCHSBM-like hypergraph model with $\bar{\ell} = n/200$ clusters and $m = 10n$ hyperedges with size k uniformly distributed between 2 and 4. Each k -edge is, with probability p_k , placed uniformly at random on any k nodes within the same cluster. Otherwise, with probability $1 - p_k$, the edge is instead placed uniformly at random on *any* set of k nodes. We use this model rather than a direct DCHSBM to avoid the computational burden of sampling edges at each k -tuple of nodes, which is prohibitive when n is large. For the purpose of performance testing, we compute estimates of the parameter vectors β and γ (in the case of AON HMLL) and the resolution parameter γ (in the case of GMLL). We emphasize that this is typically not possible in practical applications, since the ground truth labels are not known. We make this choice in order to focus on a direct comparison runtimes of each algorithm in a situation in which both can succeed. In later sections, we study the ability of HMLL and GMLL to recover known groups in synthetic and empirical data when affinities and resolution parameters are not known.

Figure 2 shows runtime, Adjusted Rand (ARI) and four are rarely (if ever) contained completely inside clusters. Thus, hyperedges of different sizes provide different signal regarding ground truth clusters. For this experiment, we implemented Graph MLL by computing a normalized clique projection, in which nodes

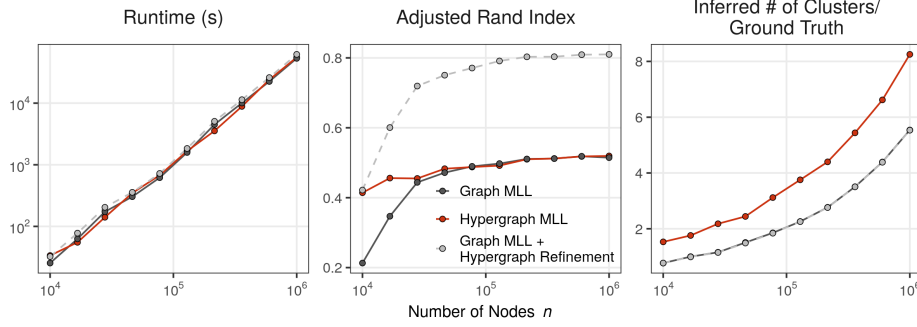


Figure 2 – Runtime, Adjusted Rand Index, and number of clusters returned by GMLL and HMLL in a synthetic testbed with optimal affinity parameters. The within-cluster edge placement probabilities are $p_2 = 3/5$, $p_3 = 1/n^3$, and $p_4 = 1/n^4$. We also show in light gray the results obtained by using GMLL as a preprocessing step, whose output partition is then refined by HMLL (light gray).

are joined by weighted dyadic edges with weights

$$w_{ij} = \sum_{e:i,j \in e} \frac{1}{|e| - 1}.$$

We also performed experiments on an unnormalized clique projection with $w_{ij} = |e : i, j \in e|$, but do not show these results because, in this experiment, the associated MLL algorithm consistently fails to recover labels correlated with the planted clusters.

On smaller instances, HMLL outperforms Graph MLL in recovering planted clusters, as measured by the ARI. For larger instances, the recovery results are comparable for larger n . Interestingly, although GMLL and HMLL obtain similar accuracy in this experiment, they do so in different ways, with HMLL tending to generate more, smaller clusters than GMLL. Importantly, the runtimes are nearly indistinguishable, indicating that dyadic clique projections are necessary neither for accuracy nor for performance. We observed other choices of the parameters p_2 , p_3 , and p_4 in which HMLL substantially outperformed GMLL in cluster recovery and vice versa; however, in each case the algorithms’ respective runtimes tended to differ by only a small constant factor.

Interestingly, in this synthetic experiment, a combination of the two algorithms leads to the strongest recovery results. In addition to running each algorithm independently, we also ran a two-stage algorithm in which GMLL is used to generate an intermediate partition, and then HMLL is used to refine it. This procedure is similar to the warmstart approach from Kamiński et al. [2020]. We emphasize again that these results are obtained on synthetic hypergraphs with pre-optimized affinity parameters, and so the effectiveness of the refinement strategy may not generalize to real data sets. Indeed, in the experiments on empirical data shown in Section 7, we do not show results from the refinement procedure because the output partition was in each case essentially indistinguishable from the output of the dyadic partition. This may reflect the fact that we did not allow the algorithms to learn *a priori* the affinity parameters associated with the true data labels. Further investigation into the performance of hybrid strategies would be of considerable practical importance.

6.2 DYADIC PROJECTIONS AND THE DETECTABILITY THRESHOLD

Informally, an algorithm is able to *detect* communities in a random graph model with fixed labels \mathbf{z} when the output labeling $\hat{\mathbf{z}}$ of that algorithm is, with probability bounded above zero, correlated with \mathbf{z} . Using arguments from statistical physics, Decelle et al. [2011] conjectured the existence of a regime in the graph stochastic blockmodel in which no algorithm can successfully detect communities. This conjecture has since been refined and proven in various special cases; see Abbe [2017] for a survey. In the dyadic stochastic blockmodel with two equal-sized

planted communities, a necessary condition for detectability is that

$$\frac{(c_i - c_o)^2}{2(c_i + c_o)} \geq 1, \quad (11)$$

where c_i is the mean number of within-cluster edges attached to a node, and c_o is the mean number of between-cluster edges attached to a node. If this condition is not satisfied, no algorithm can reliably detect communities in the associated graph stochastic blockmodel. This bound limits both direct inferential methods, such as Bayesian or maximum-likelihood techniques, as well as methods based on maximization of modularity or other graph objectives [Nadakuditi and Newman, 2012]. Several recent papers have considered the detectability problem in the case of uniform hypergraphs [Ghoshdastidar and Dukkipati, 2014, 2017; Angelini et al., 2016]. In our model, the presence of edges of multiple sizes complicates analysis. Here, we limit ourselves to an experimental demonstration that the regimes of detectability for the graph SBM and our DCHSBM can differ significantly.

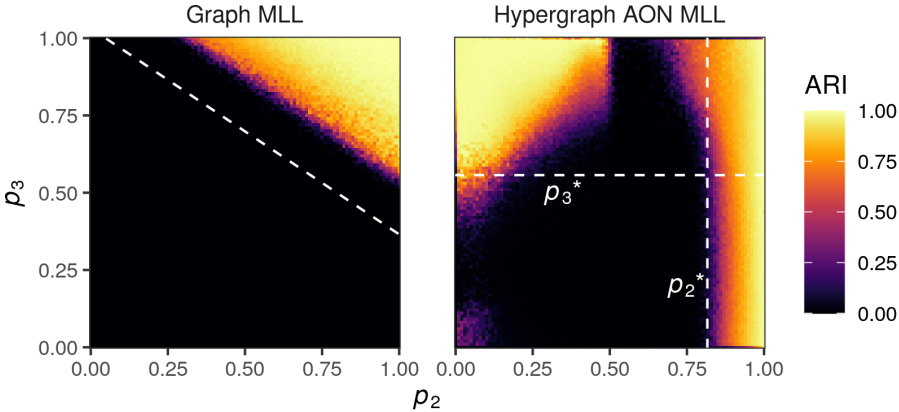


Figure 3 shows two experiments on a simple DCHSBM with two equal-sized communities of 250 nodes each. The affinity Ω is tuned so that:

1. Each node is incident to, on average, five 2-edges and five 3-edges.
2. A fraction p_2 of 2-edges join nodes in the same cluster, while a fraction $1 - p_2$ of 2-edges join nodes in different clusters.
3. A fraction p_3 of 3-edges join nodes in the same cluster, while a fraction $1 - p_3$ of 3-edges join nodes in different clusters.

In the left panel, we show the Adjusted Rand Index (ARI) of the returned partition $\hat{\mathbf{z}}$ against the true partition \mathbf{z} when using the unnormalized variant of GMLL (results for the normalized variant are similar). There is a gap between the theoretical bound (dashed white line) given by (11) and the regime in which GMLL is able to find partitions correlated with the planted ones. This reflects the fact that the Louvain algorithm, as a stagewise greedy method, possesses no optimality guarantees.

In the right panel, we show the same experiment using AON HMLL. HMLL is able to detect the planted partition for a range of parameter values in which GMLL is not. These include the case in which edges of certain sizes are largely between-cluster, as shown in the top left (small p_2) and bottom right (small p_3). There is a regime (mid and bottom right) in which the algorithm appears to be constrained by a threshold p_2^* , which represents the detectability threshold for a dyadic algorithm when 3-edges are ignored. This suggests that HMLL is effectively

Figure 3 – Detectability experiments in synthetic hypergraphs. For $i = 2, 3$, p_i is the proportion of within-cluster edges of size i . Each pixel gives the mean ARI over 20 independently generated DCHSBMs of size $n = 500$ where each node is incident to, on average, five 2-edges and five 3-edges. (Left) The recovered partition $\hat{\mathbf{z}}$ is obtained from GMLL. The dashed white line gives the detectability threshold for a dyadic algorithm with the same within- and between-cluster average as the clique projection. (Right) The recovered partition is obtained from AON HMLL (Algorithm 3). The dashed line p_2^* gives the detectability threshold in p_2 for a dyadic algorithm that ignores 3-edges. The dashed line p_3^* gives the same threshold in p_3 for a dyadic algorithm that ignores 2-edges. The returned partition $\hat{\mathbf{z}}$ is highest-likelihood partition from 20 alternations between updating $\hat{\mathbf{z}}$ and inference of the affinity parameters.

ignoring 3-edges in this regime. As p_3 increases, however, 3-edges become more informative and the partition can be detected for some values $p_2 < p_2^*$ (top right). There is also a broad regime (top left) in which the hypergrph algorithm is able effectively to use both 2- and 3-edges to detect clusters, even when 2-edges are disassortative. This regime is largely inaccessible to GMLL. Intriguingly, there are also values of p_2 and p_3 in which GMLL is able to detect the planted partition while HMLL is not. This may indicate that the pooling of edges of different sizes implied by the dyadic projection can be useful in some regimes. We note again that neither GMLL or HMLL are optimal inference algorithms. An optimal hypergraph algorithm might significantly extend the detectable regime in the right panel of Figure 3. We pose the development of such algorithms, as well as its analysis, as highly promising avenues for future research.

7 EXPERIMENTS WITH EMPIRICAL DATA

Next, we analyze several hypergraphs derived from empirical data. The first two are hypergraphs of human close-proximity contact interactions [Benson et al., 2018], obtained from wearable sensor data at a primary school [Stehlé et al., 2011] and a high school [Mastrandrea et al., 2015]. Nodes are students or teachers, and a hyperedge connects groups of people that were all jointly in proximity to one another. Node labels identify the classrooms to which each student belongs, and the primary school data also includes a teacher associated to each class. Next, we created two hypergraphs from U.S. Congressional bill cosponsorship data [Fowler, 2006a,b], where nodes correspond to congresspersons, and hyperedges correspond to the sponsor and all cosponsors of a bill in either the House of Representatives or the Senate. We constructed another pair of data sets from the U.S. Congress in the form of committee memberships [Stewart and Woon, 2021]. Each edge is a committee in a meeting of Congress, and each node again corresponds to a member of the House or a senator. A node is contained in an edge if the corresponding legislator was a member of the committee during the specified meeting of Congress. The 103rd through 115th Congresses are represented, spanning the years 1993–2017. There are again separate data sets for House and Senate members. In all congressional data sets, the node labels give the political parties of the members. We also used a hypergraph of Walmart purchases [Amburg et al., 2020], where each node is a product and a hyperedge connects a set of products that were co-purchased by a customer in a single shopping trip. Each node has an associated product category label. Finally, we constructed a hypergraph where nodes correspond to hotels listed at trivago.com, and each hyperedge corresponds to a set of hotels whose web site was clicked on by a user of Trivago within a browsing session. This hypergraph was derived from data released for the 2019 ACM RecSys Challenge contest.⁵ For each hotel, the node label gives the country in which it is located. The data sets vary in size in terms of the number of nodes, hyperedges, hyperedge sizes, and node labels (Table 4).

	n	m	$\langle d \rangle$	$s(d)$	$\langle k \rangle$	$s(k)$	$\bar{\ell}$
contact-primary-school	242	12,704	127.0	55.3	2.4	0.6	11
contact-high-school	327	7,818	55.6	27.1	2.3	0.5	9
house-bills	1,494	43,047	274.0	282.7	9.5	7.2	2
senate-bills	293	20,006	493.4	406.3	7.3	5.5	2
house-committees	1,290	340	9.2	7.1	35.2	21.3	2
senate-committees	282	315	19.0	14.7	17.5	6.6	2
walmart-purchases	88,860	65,979	5.1	26.7	6.7	5.3	11
trivago-clicks	171,495	220,758	4.0	7.0	4.2	2.0	160

⁵ <https://recsys.acm.org/recsys19/challenge/>

Table 4 – Summary of study data sets. Shown are the number of nodes n , number of hyperedges m , mean degree $\langle d \rangle$, standard deviation of degree $s(d)$, mean edge size $\langle k \rangle$, standard deviation of edge size $s(k)$, and number of data labels $\bar{\ell}$.

7.1 MODEL COMPARISON AND HIGHER-ORDER STRUCTURE

It is often stated that higher-order features are important for understanding the structure and function of complex networks. It is less often clarified what *kinds* of higher-order features are relevant *for which* networks. Generative modeling provides one way to compare different kinds of higher-order structure. In the DCHSBM, this structure is specified by the affinity function Ω . Comparison of the likelihood functions obtained by each affinity can indicate which one is most plausible as a higher-order generative mechanism of the underlying data. We performed such a comparison using the symmetric affinity functions from Table 1 and the labels for nodes described above; in this setup, we can compute the optimal Ω estimate, given its functional form. In order to make concrete comparisons, it is necessary to specify the functional forms of the Group Number (GN), Relative Plurality (RP), and Pairwise (P) affinities. We use the following parameterizations:

$$\begin{aligned}\Omega(\mathbf{p}) &= \omega_{\|p\|_0, k} && \text{(Group Number)} \\ \Omega(\mathbf{p}) &= \begin{cases} \omega_{k1} & p_1 - p_2 < \frac{k}{4} \\ \omega_{k0} & \text{otherwise} \end{cases} && \text{(Relative Plurality)} \\ \Omega(\mathbf{p}) &= \begin{cases} \omega_{k1} & \sum_{i \neq j} p_i p_j < \frac{k(k-1)}{4} \\ \omega_{k0} & \text{otherwise} \end{cases} && \text{(Pairwise)}\end{aligned}$$

The Group Number affinity function assigns a separate parameter to each combination of edge size and number of groups. The Relative Plurality affinity function assigns one parameter for the case that the difference between the largest and second largest groups within an edge exceeds $k/4$, where k is the size of the edge. The Pairwise affinity function assigns one parameter to the case that the total number of dyadic pairs in differing groups exceeds half the possible number of such pairs. Different parameterizations of these symmetric affinities are possible, which may generate slightly different results. Because these affinity functions possess different numbers of parameters, we measure the approximate Bayesian Information Criterion (BIC) [Schwarz, 1978], which penalizes affinity functions with more parameters than are supported by the data.

Table 5 shows the BIC for the DCHSBM using each of these affinity functions. Importantly, no single affinity function is preferred across all of the study data sets, suggesting the presence of different kinds of polyadic structure. AON, GN, and P all prefer edges with homogeneous cluster labels, whereas RP prefers edges in which the two most common labels are roughly balanced in representation. In the two congressional committee data sets, RP achieves the optimal BIC, while in each of the other data sets, one of the three affinities that promotes edge homogeneity is instead preferred. There are also important differences between these three affinities. In `house-bills`, the Pairwise affinity function achieves the lowest BIC overall, while in `walmart-purchases` the Pairwise affinity is preferred over all but the Group Number affinity. This suggests that a model involving only pairwise comparison of node labels can provide relatively strong generative explanations of the data in these cases. This in turn suggests that dyadic algorithms may perform at least as well on these data sets as their polyadic counterparts. Indeed, as we will see below, in both of these data sets, dyadic algorithms can return clusterings more correlated with ground truth than those returned by AON HMLL.

7.2 RECOVERING CLASSES IN CONTACT HYPERGRAPHS

To test the AON HMLL algorithm itself, we first studied its behavior in the `contact-primary-school` and `contact-high-school` networks. The comparison of BIC scores from Table 5 suggests that GN may be the most explanatory model of the data, but we instead use AON in order to take advantage of its considerable computational benefits. We performed 20 alternations between AON HMLL and

	AON	GN	RP	P	
contact-high-school	2.2003	2.1946	2.4330	2.2003	$\times 10^5$
contact-primary-school	4.1954	4.1646	4.3990	4.1954	$\times 10^5$
house-committees	2.7128	2.7128	2.7119	2.7127	$\times 10^5$
senate-committees	9.7934	9.7934	9.7736	9.7933	$\times 10^4$
house-bills	9.9719	9.9720	10.003	9.9670	$\times 10^6$
senate-bills	3.1925	3.1926	3.2030	3.1925	$\times 10^6$
walmart-purchases	1.0763	1.0753	1.0806	1.0758	$\times 10^6$
trivago-clicks	1.6854	1.6866	2.0257	1.6960	$\times 10^8$

Table 5 – Bayesian Information Criteria (BIC) of the DCHSBM using the the All-Or-Nothing (AON), Group Number (GN), Relative Plurality (RP), and Pairwise (P) affinity functions on our study data sets. Definitions of each affinity function are supplied in Table 1. Lower BIC indicates a more plausible model. The affinity function achieving the lowest BIC in each data set is shown in **bold**.

estimation of the AON parameters, and returned the partition with the highest DCHSBM likelihood. We compare the results to two dyadic methods. Each step of the Graph Louvain algorithm alternates between using the standard Louvain algorithm [Blondel et al., 2008] to infer clusters and estimating the resolution parameter γ using the approximate maximum-likelihood framework of [Newman, 2016]. Graph Louvain returns the partition which maximizes the classical dyadic modularity objective. We also compare to Graph Maximum-Likelihood Louvain (GMLL), which carries out the same alternation, but instead returns the partition that maximizes the approximate log-likelihood of the corresponding planted partition stochastic blockmodel.

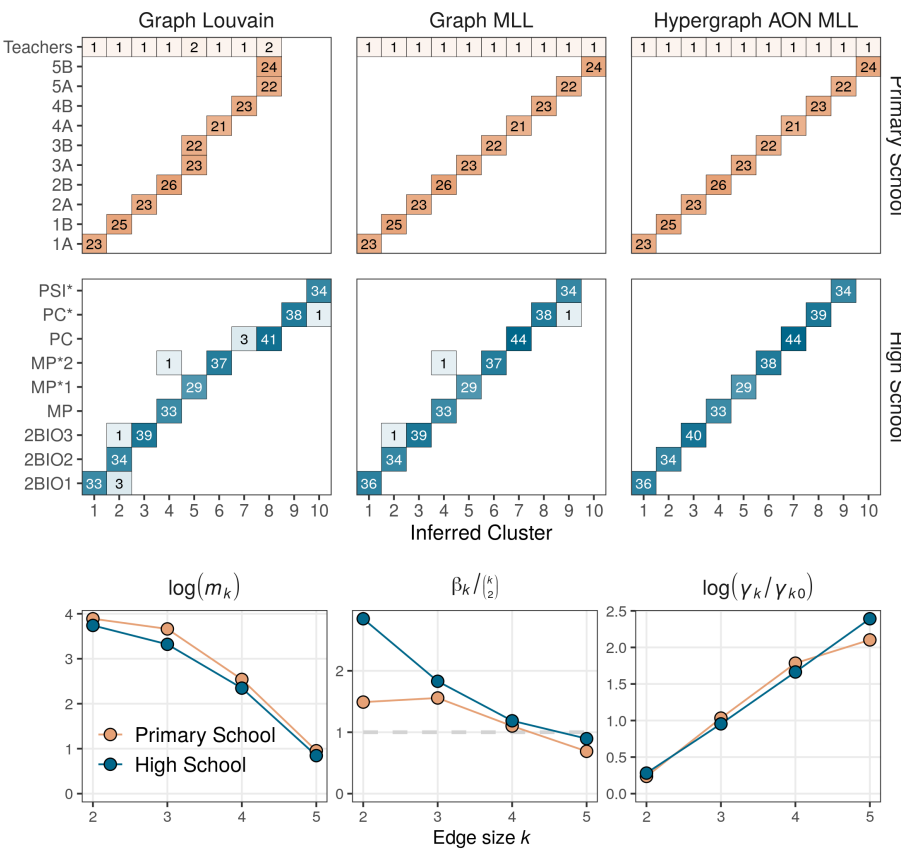


Figure 6 – Comparison of clustering algorithms in contact-primary-school and contact-high-school. For each data set, we show a partition obtained from the classical graph Louvain modularity maximization heuristic; a partition obtained from Graph Maximum-Likelihood Louvain (GMLL); and partition obtained by AON HMLL. The partition shown is the one which attains the corresponding objective function after 20 rounds of iterative likelihood maximization. Each box records the number of agents with the specified combination of inferred cluster and ground truth label. The bottom row visualizes the number m_k of edges of size k , the inferred size weights β_k , and inferred resolution parameters γ_k as defined in (10). On the far right, $\gamma_{k0} = m_k / \text{vol}(H)^k$.

Figure 6 compares the performance of each of these algorithms. In the case of **contact-primary-school**, we consider the ground truth partition to be the one that assigns exactly one teacher to each class. Graph Louvain is able to find partitions of students with clear correlations with the given class labels, but conflates two primary school classes and splits several high school classes (left column, top two

rows). Graph MLL is able to perfectly recover the primary school student class labels, and misclassifies three high school students. Our proposed AON HMLL is able to correctly recover the given partitions in both data sets.

We can obtain some qualitative insight into the behavior of HMLL by studying the structure of the inferred affinity function Ω . The most intuitive way to do so is by considering the derived parameters β_k and γ_k from (10). The bottom row of Figure 6 shows these parameters, as well as the distribution of edge sizes. The dependence of β_k on edge size k provides one explanation of why Graph MLL succeeds in `contact-primary-school` but makes several errors in `contact-high-school`. Under the standard dyadic projection, a k -hyperedge generates $\binom{k}{2}$ 2-edges, and therefore appears in the dyadic modularity objective $\binom{k}{2}$ distinct times. In the case of `contact-primary-school`, the estimated importance parameter β_k is indeed relatively close to $\binom{k}{2}$ (bottom center panel of Figure 6). At the optimal partition, the relative weights of edges are therefore distorted relatively little by the clique projection. On the other hand, the estimates for β_k in `contact-high-school` deviate considerably from $\binom{k}{2}$, especially for $k = 2, 3$. Here, small edges feature much more prominently in the polyadic modularity objective than they do in the projected dyadic objective, implying that the latter is a poorer approximation to the former near the optimal partition. This difference may explain the small errors in Graph MLL in `contact-high-school`. The bottom-right panel of Figure 6 compares the inferred value of the size-specific resolution parameter γ_k to $\gamma_{k0} = m_k / \text{vol}(H)^k$, the implicit value used in [Kamiński et al., 2019]. The inferred resolution parameters are consistently larger γ_{k0} and increase with k , highlighting the value of adaptively estimating these parameters in our approach.

7.3 CLUSTER RECOVERY WITH LARGE HYPEREDGES

In Figure 7, we study the ability of AON HMLL to recover ground truth communities in several more of our study data sets. Unlike the two contact networks, each of these data sets contains edges of size up to 25 nodes. We have excluded `house-committees` and `senate-committees` on the grounds that these data sets are *disassortative*, indicating that AON is clearly inappropriate. We compare AON HMLL to two variants of GMML. In the unnormalized variant, we obtain a dyadic graph by replacing each k -edge with a k -clique, thus generating a total of $\binom{k}{2}$ dyadic edges. In the normalized variant, we weight each edge in the k -clique by a factor of $\frac{1}{k-1}$. The normalized dyadic degree of each node is then equal to its degree in the original hypergraph. In either case, we then alternate between the dyadic Louvain algorithm for estimating clusters and maximum-likelihood inference of the resolution parameter γ . In each trial, we perform 20 iterations of AON HMLL as well as the two GMML variants, returning from these the combination of group labels and parameters that achieves the highest likelihood. We then compare the clustering to the ground truth labels via the Adjusted Rand Index. We vary the maximum edge size \bar{k} in order to show how each algorithm responds to the incorporation of progressively larger edges. Because extreme sparsity poses issues for community detection algorithms in general [Abbe, 2017], we show experiments for progressively denser cores of `trivago-clicks` and `walmart-purchases`.

The results highlight the strong dependence of the performance of AON HMLL on the relative plausibility of the AON affinity function as a generative mechanism for the data (cf. Table 5). In `trivago-clicks`, the AON affinity function achieved the lowest BIC of all four candidates. Because AON is a more plausible generating mechanism, it is not surprising that AON HMLL is able to find partitions considerably more correlated with the supplied data labels than those returned by the dyadic variants. In `walmart-purchases`, on the other hand, the Pairwise affinity is preferred to AON. In this case, AON HMLL performs much worse, and in the 2-core even returns clusters which are anticorrelated with the supplied labels. As weakly-connected nodes are removed and the resulting

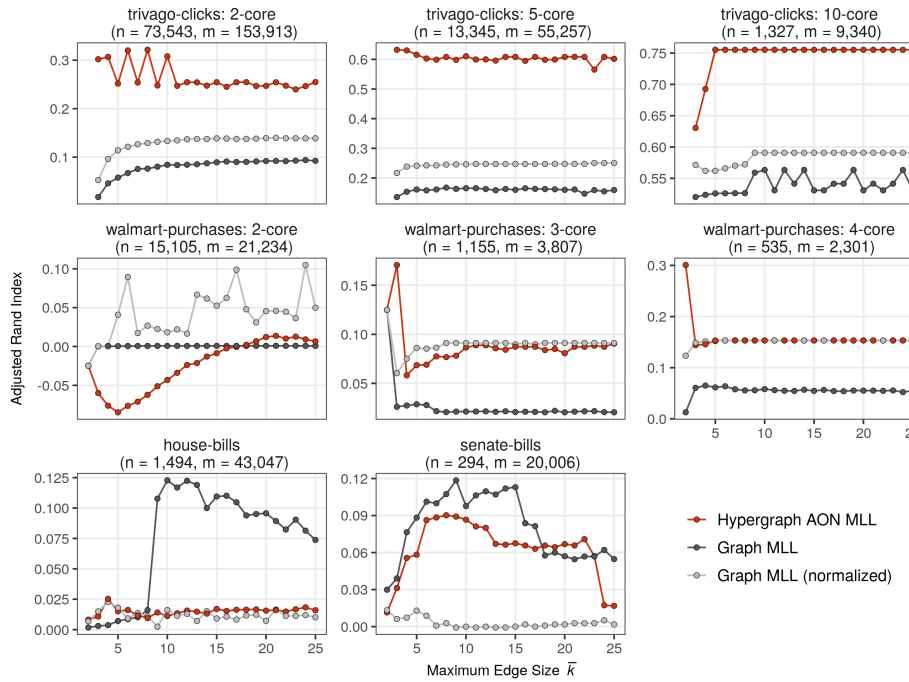


Figure 7 – Comparison of Hypergraph All-Or-Nothing MLL Algorithm 3 against dyadic likelihood Louvain in data with known clusters. Points give the Adjusted Rand Index of the highest-likelihood partition obtained after 20 alternations between partitioning and parameter estimation. The maximum edge size \bar{k} varies along the horizontal axis. In the panel titles, n is the number of nodes and m the number of edges when $\bar{k} = 25$. Note that the vertical axis limits vary between panels.

data becomes denser, HMLL begins to return correlated clusters. However, the normalized GMLL variant is at least as effective in recovering the data labels. In the two Congressional bills data sets, the Pairwise affinity achieves a lower BIC than AON in the House and a comparable one in the Senate. It is therefore not surprising that a dyadic method outperforms AON HMLL in each of these cases. Interestingly, unnormalized GMLL performs best in `house-bills` and `senate-bills`, while normalized GMLL is preferable in `walmart-purchases`. In addition, HMLL is the worst algorithm only in the case of the 2-core of `walmart-purchases` for small \bar{k} . HMLL may therefore be the algorithm of choice in cases when it is not known whether normalized or unnormalized dyadic representations are more appropriate for the data.

When interpreting these recovery results, it is important to contextualize them within the limitations of community detection methods in general and of modularity maximization in particular. There is no “best algorithm” for community detection that does not make implicit assumptions about the structure of the data, and mismatch of algorithms to data sets can generate misleading results [Peel et al., 2017].⁶ Even when the data generating process indeed matches algorithmic assumptions—such as a synthetic data set generating from a stochastic blockmodel—even optimal algorithms may fail to detect planted communities due to sparsity [Decelle et al., 2011; Abbe, 2017]. Greedy modularity maximization, such as in the Louvain variants considered here, only finds one of possibly many local optima [Good et al., 2010], some of which may be largely uncorrelated with each other. These considerations imply that (a) we cannot rule out the existence of other local optima which might achieve higher scores in any of the three algorithms and (b) the fact that an algorithm fails to recover a clustering close to the ground truth does not imply that it is “failing” in its stated objective, namely, local likelihood maximization. Overall, our results suggest that, when the assumptions of the DCHSBM with All-Or-Nothing affinity are appropriate to the data, AON HMLL can outperform dyadic approaches in recovering ground truth communities. In practice, since we often do not have access to ground truth labels, the question of whether or not the assumptions are appropriate to the

⁶ That being said, a test similar to BESTest [Peel et al., 2017] reveals that the likelihood under DCHSBM is much greater than the likelihood under random label permutations in most data set configurations, implying significant correlation between network structure and the labels.

data should be informed by domain expertise.

8 DISCUSSION

We have proposed a generative approach for clustering polyadic data, grounded in a degree-corrected hypergraph stochastic blockmodel. From this model we derived a symmetric, modularity-like objective, which includes the All-Or-Nothing (AON) modularity objective as an important special case. Theoretically, our approach connects hypergraph modularity objectives to concrete modeling assumptions, which can be tuned in response to domain expertise. We have also formulated Louvain-like algorithms for optimizing these objectives, which are highly scalable in the case of the AON affinity function. By embedding this heuristic within an alternating approximate maximum-likelihood scheme, we are able to adaptively learn both node clusters and affinity parameters. We showed experimentally that hypergraph algorithms possess markedly different detectability regimes from dyadic algorithms. We also conducted experiments on empirical data, finding that hypergraph methods are preferred to dyadic ones in data sets where their modeling assumptions are well-founded.

Our work points toward many directions of further research. One of these directions is algorithmic. Our greedy coordinate-ascent framework for inference in the DCHSBM has several important limitations. First, because we rely on an NP-hard optimization step, global maximization of the likelihood is never assured. Second, exact maximum-likelihood itself is limited as an inference paradigm, as it uses information contained only within a small part of the likelihood landscape. Our method, as an approximation which is exact only when clusters are of roughly equal sizes, may also suffer from estimation bias induced by the approximation. Third, the edgewise agglomerative approach embodied by Louvain-style algorithms is limited in applicability to affinity functions that promote homogeneity within edges. Alternative inference paradigms may ameliorate some or all of these limitations. Fully Bayesian treatments [Peixoto, 2019] provide one promising path, although these are sometimes limited in their computational scalability. Variational belief-propagation [Decelle et al., 2011; Zhang and Moore, 2014] provides an intriguing compromise, achieving considerable scalability in exchange for several approximations. A derivation of such an algorithm, and an exploration into the applicability of the belief-propagation approximations in hypergraph data, would be of considerable interest. Methods enabling scalable inference with more general affinity functions would be of special practical importance.

There are also several important directions of theoretical development. One of these is the question of detectability in the DCHSBM. Because the DCHSBM is more flexible than the dyadic DCSBM, the theory of detectability in this model may be substantially more complex. Another direction concerns the properties of the dyadic modularity objective that extend to the hypergraph modularity objectives discussed here. In addition to its role as a comparison against null models [Newman, 2006] and as a term in the DCSBM likelihood [Newman, 2016], the dyadic modularity also expresses the stability of diffusion processes on graphs [Delvenne et al., 2010] and the energy of discrete surface tensions defined on graphs [Boyd et al., 2019]. Extensions of these properties, or explanations of why they fail to generalize, would be helpful for both theorists and practitioners.

ACKNOWLEDGMENTS

We are grateful to Tiago de Paula Peixoto for pointing out the distinction between exact and approximate maximum-likelihood estimation of θ discussed at the end of Section 4.1.

FUNDING

This research was supported in part by ARO Award W911NF19-1-0057, ARO MURI, NSF Award DMS-1830274, and JP Morgan Chase & Co.

SOFTWARE AND DATA

Software and data sufficient to reproduce and extend the experiments and analysis in this paper are available at the following repository:

<https://github.com/PhilChodrow/HypergraphModularity>.

The data are also hosted in packaged format at

<https://www.cs.cornell.edu/~arb/data/#hyperlabels>.

REFERENCES

[Abbe, 2017] E. ABBE. *Community detection and stochastic block models: recent developments*. The Journal of Machine Learning Research, 18 (1), pp. 6446–6531, 2017. Cited on pages 3, 14, 19, and 20.

[Agarwal et al., 2006] S. AGARWAL, K. BRANSON, and S. BELONGIE. *Higher order learning with graphs*. In *Proceedings of the 23rd International Conference on Machine Learning*, pp. 17–24. 2006. doi:10.1145/1143844.1143847. Cited on page 4.

[Agarwal et al., 2005] S. AGARWAL, J. LIM, L. ZELNIK-MANOR, P. PERONA, D. KRIEGMAN, and S. BELONGIE. *Beyond pairwise clustering*. In *Proceedings of the 2005 IEEE Computer Society Conference on Computer Vision and Pattern Recognition (CVPR'05) - Volume 2 - Volume 02*, pp. 838–845. 2005. doi:10.1109/CVPR.2005.89. Cited on page 2.

[Airoldi et al., 2008] E. M. AIROLDI, D. M. BLEI, S. E. FIENBERG, and E. P. XING. *Mixed membership stochastic blockmodels*. Journal of Machine Learning Research, 9 (Sep), pp. 1981–2014, 2008. Cited on pages 2 and 7.

[Akremtsev et al., 2017] Y. AKHREMSEV, T. HEUER, P. SANDERS, and S. SCHLAG. *Engineering a direct k-way hypergraph partitioning algorithm*. In *19th Workshop on Algorithm Engineering and Experiments, (ALENEX 2017)*, pp. 28–42. 2017. Cited on page 4.

[Amburg et al., 2020] I. AMBURG, N. VELDT, and A. BENSON. *Clustering in graphs and hypergraphs with categorical edge labels*. In *Proceedings of The Web Conference 2020*, pp. 706–717. 2020. Cited on pages 2 and 16.

[Angelini et al., 2016] M. C. ANGELINI, F. CALTAGIRONE, F. KRZAKALA, and L. ZDEBOROVÁ. *Spectral detection on sparse hypergraphs*. 2015 53rd Annual Allerton Conference on Communication, Control, and Computing, Allerton 2015, pp. 66–73, 2016. arXiv:1507.04113, doi:10.1109/ALLERTON.2015.7446987. Cited on page 15.

[Athreya et al., 2017] A. ATHREYA, D. E. FISHKIND, M. TANG, C. E. PRIEBE, Y. PARK, J. T. VOGELSTEIN, K. LEVIN, V. LYZINSKI, and Y. QIN. *Statistical inference on random dot product graphs: a survey*. The Journal of Machine Learning Research, 18 (1), pp. 8393–8484, 2017. Cited on page 2.

[Ballard et al., 2016] G. BALLARD, A. DRUINSKY, N. KNIGHT, and O. SCHWARTZ. *Hypergraph partitioning for sparse matrix-matrix multiplication*. ACM Transactions on Parallel Computing, 3 (3), pp. 18:1–18:34, 2016. doi:10.1145/3015144. Cited on page 2.

[Barber, 2007] M. J. BARBER. *Modularity and community detection in bipartite networks*. Physical Review E, 76 (6), p. 066102, 2007. Cited on page 5.

[Battiston et al., 2020] F. BATTISTON, G. CENCETTI, I. IACOPINI, V. LATORA, M. LUCAS, A. PATANIA, J.-G. YOUNG, and G. PETRI. *Networks beyond pairwise interactions: structure and dynamics*. Physics Reports, 2020. Cited on page 1.

[Benson et al., 2018] A. R. BENSON, R. ABEBE, M. T. SCHAUB, A. JADBABAIE, and J. KLEINBERG. *Simplicial closure and higher-order link prediction*. Proceedings of the National Academy of Sciences, 2018. doi:10.1073/pnas.1800683115. Cited on pages 1, 2, and 16.

[Benson et al., 2016] A. R. BENSON, D. F. GLEICH, and J. LESKOVEC. *Higher-order organization of complex networks*. Science, 353 (6295), pp. 163–166, 2016. doi:10.1126/science.aad9029. Cited on pages 1, 2, and 4.

[Blondel et al., 2008] V. D. BLONDEL, J.-L. GUILLAUME, R. LAMBIOTTE, and E. LEFEBVRE. *Fast unfolding of communities in large networks*. Journal of Statistical Mechanics: Theory and Experiment, 2008 (10), p. P10008, 2008. Cited on pages 3, 5, 11, and 18.

[Bolla, 1993] M. BOLLA. *Spectra, euclidean representations and clusterings of hypergraphs*. Discrete Math., 117 (1-3), pp. 19–39, 1993. doi:10.1016/0012-365X(93)90322-K. Cited on page 4.

[Boyd et al., 2019] Z. M. BOYD, M. A. PORTER, and A. L. BERTOZZI. *Stochastic block models are a discrete surface tension*. Journal of Nonlinear Science, pp. 1–34, 2019. Cited on page 21.

[Brandes et al., 2007] U. BRANDES, D. DELLING, M. GAERTLER, R. GÖRKE, M. HOEFER, Z. NIKOLOSKI, and D. WAGNER. *On finding graph clusterings with maximum modularity*. In *International Workshop on Graph-Theoretic Concepts in Computer Science*, pp. 121–132. 2007. Cited on pages 3 and 5.

[Chan et al., 2018] T.-H. H. CHAN, A. LOUIS, Z. G. TANG, and C. ZHANG. *Spectral properties of hypergraph laplacian and approximation algorithms*. J. ACM, 65 (3), 2018. doi:10.1145/3178123. Cited on page 4.

[Chang et al., 2020] J. CHANG, Y. CHEN, L. QI, and H. YAN. *Hypergraph clustering using a new laplacian tensor with applications in image processing*. SIAM Journal on Imaging Sciences, 13 (3), pp. 1157–1178, 2020. doi:10.1137/19M1291601. Cited on page 4.

[Chen et al., 2017] Y. CHEN, L. QI, and X. ZHANG. *The fiedler vector of a laplacian tensor for hypergraph partitioning*. SIAM Journal on Scientific Computing, 39 (6), pp. A2508–A2537, 2017. doi:10.1137/16M1094828. Cited on page 4.

[Chodrow, 2020a] P. S. CHODROW. *Configuration models of random hypergraphs*. Journal of Complex Networks, 8 (3), p. cnaa018, 2020a. Cited on page 2.

[Chodrow, 2020b] ———. *Moments of uniform random multigraphs with fixed degree sequences*. SIAM Journal on Mathematics of Data Science, 2 (4), pp. 1034–1065, 2020b. Cited on page 5.

[Chung and Lu, 2002] F. CHUNG and L. LU. *Connected components in random graphs with given expected degree sequences*. Annals of combinatorics, 6 (2), pp. 125–145, 2002. Cited on page 6.

[Chung, 1992] F. R. L. CHUNG. *Spectral Graph Theory*, American Mathematical Society, 1992. Cited on page 4.

[Clauset et al., 2004] A. CLAUSET, M. E. NEWMAN, and C. MOORE. *Finding community structure in very large networks*. Physical Review E, 70 (6), p. 066111, 2004. Cited on page 6.

[Condon and Karp, 2001] A. CONDON and R. M. KARP. *Algorithms for graph partitioning on the planted partition model*. Random Structures & Algorithms, 18 (2), pp. 116–140, 2001. Cited on pages 2 and 9.

[de Arruda et al., 2020] G. F. DE ARRUDA, G. PETRI, and Y. MORENO. *Social contagion models on hypergraphs*. Physical Review Research, 2 (2), p. 023032, 2020. Cited on page 1.

[Decelle et al., 2011] A. DECELLE, F. KRZAKALA, C. MOORE, and L. ZDEBOROVÁ. *Asymptotic analysis of the stochastic block model for modular networks and its algorithmic applications*. Physical Review E, 84 (6), p. 066106, 2011. Cited on pages 7, 14, 20, and 21.

[Delvenne et al., 2010] J.-C. DELVENNE, S. N. YALIRAKI, and M. BARAHONA. *Stability of graph communities across time scales*. Proceedings of the National Academy of Sciences, 107 (29), pp. 12755–12760, 2010. Cited on pages 5 and 21.

[Deveci et al., 2015] M. DEVECI, K. KAYA, B. UÇAR, and ÜMIT V. ÇATALYÜREK. *Hypergraph partitioning for multiple communication cost metrics: Model and methods*. Journal of Parallel and Distributed Computing, 77, pp. 69 – 83, 2015. doi: 10.1016/j.jpdc.2014.12.002. Cited on page 10.

[Easley and Kleinberg, 2010] D. EASLEY and J. KLEINBERG. *Networks, crowds, and markets: Reasoning about a highly connected world*, Cambridge University Press, 2010. Cited on page 1.

[Expert et al., 2011] P. EXPERT, T. S. EVANS, V. D. BLONDEL, and R. LAMBIOTTE. *Uncovering space-independent communities in spatial networks*. Proceedings of the National Academy of Sciences, 108 (19), pp. 7663–7668, 2011. Cited on page 5.

[Fortunato and Barthelemy, 2007] S. FORTUNATO and M. BARTHELEMY. *Resolution limit in community detection*. Proceedings of the National Academy of Sciences, 104 (1), pp. 36–41, 2007. Cited on page 5.

[Fortunato and Hric, 2016] S. FORTUNATO and D. HRIC. *Community detection in networks: A user guide*. Physics Reports, 659, pp. 1–44, 2016. Cited on page 2.

[Fosdick et al., 2018] B. K. FOSDICK, D. B. LARREMORE, J. NISHIMURA, and J. UGANDER. *Configuring random graph models with fixed degree sequences*. SIAM Review, 60 (2), pp. 315–355, 2018. Cited on page 5.

[Fowler, 2006a] J. H. FOWLER. *Connecting the congress: A study of cosponsorship networks*. Political Analysis, pp. 456–487, 2006a. Cited on page 16.

[Fowler, 2006b] ———. *Legislative cosponsorship networks in the us house and senate*. Social Networks, 28 (4), pp. 454–465, 2006b. Cited on page 16.

[Ghoshdastidar and Dukkipati, 2014] D. GHOSHDASTIDAR and A. DUKKIPATI. *Consistency of spectral partitioning of uniform hypergraphs under planted partition model*. In *Advances in Neural Information Processing Systems*, pp. 397–405. 2014. Cited on pages 2, 4, and 15.

[Ghoshdastidar and Dukkipati, 2017] ———. *Consistency of spectral hypergraph partitioning under planted partition model*. Annals of Statistics, 45 (1), pp. 289–315, 2017. arXiv:1505.01582, doi:10.1214/16-AOS1453. Cited on page 15.

[Gleich and Mahoney, 2016] D. F. GLEICH and M. W. MAHONEY. *Mining large graphs*. In *Handbook of Big Data*. CRC Press, 2016. Cited on page 10.

[Good et al., 2010] B. H. GOOD, Y.-A. DE MONTJOYE, and A. CLAUSET. *Performance of modularity maximization in practical contexts*. Physical Review E, 81 (4), p. 046106, 2010. Cited on pages 5 and 20.

[Guimerà et al., 2007] R. GUIMERÀ, M. SALES-PARDO, and L. A. N. AMARAL. *Module identification in bipartite and directed networks*. Physical Review E, 76 (3), p. 036102, 2007. Cited on page 5.

[Hendrickson and Kolda, 2000] B. HENDRICKSON and T. G. KOLDA. *Graph partitioning models for parallel computing*. Parallel computing, 26 (12), pp. 1519–1534, 2000. Cited on page 10.

[Hoff et al., 2002] P. D. HOFF, A. E. RAFTERY, and M. S. HANDCOCK. *Latent space approaches to social network analysis*. Journal of the American Statistical Association, 97 (460), pp. 1090–1098, 2002. Cited on page 2.

[Jackson, 2008] M. O. JACKSON. *Social and Economic Networks*, Princeton University Press, 2008. Cited on page 1.

[Jerrum and Sorkin, 1998] M. JERRUM and G. B. SORKIN. *The metropolis algorithm for graph bisection*. Discrete Applied Mathematics, 82 (1-3), pp. 155–175, 1998. Cited on pages 2 and 9.

[Kabiljo et al., 2017] I. KABILJO, B. KARRER, M. PUNDIR, S. PUPYREV, and A. SHALITA. *Social hash partitioner: a scalable distributed hypergraph partitioner*. Proceedings of the VLDB Endowment, 10 (11), pp. 1418–1429, 2017. Cited on pages 2 and 10.

[Kamiński et al., 2019] B. KAMIŃSKI, V. POULIN, P. PRALAT, P. SZUFEL, and F. THÉBERGE. *Clustering via hypergraph modularity*. PLoS ONE, 14 (11), p. e0224307, 2019. Cited on pages 3, 6, 11, and 19.

[Kamiński et al., 2020] B. KAMIŃSKI, P. PRALAT, and F. THÉBERGE. *Community detection algorithm using hypergraph modularity*. In *International Conference on Complex Networks and Their Applications*, pp. 152–163. 2020. Cited on page 14.

[Karrer and Newman, 2011] B. KARRER and M. E. NEWMAN. *Stochastic blockmodels and community structure in networks*. Physical Review E, 83 (1), p. 016107, 2011. Cited on pages 2, 3, and 6.

[Karypis et al., 1999] G. KARYPIS, R. AGARWAL, V. KUMAR, and S. SHEKHAR. *Multilevel hypergraph partitioning: applications in vlsi domain*. IEEE Transactions on Very Large Scale Integration (VLSI) Systems, 7 (1), pp. 69–79, 1999. doi:10.1109/92.748202. Cited on pages 2 and 4.

[Karypis and Kumar, 2000] G. KARYPIS and V. KUMAR. *Multilevel k-way hypergraph partitioning*. VLSI design, 11 (3), pp. 285–300, 2000. Cited on pages 4 and 10.

[Ke et al., 2019] Z. T. KE, F. SHI, and D. XIA. *Community detection for hypergraph networks via regularized tensor power iteration*. arXiv preprint arXiv:1909.06503, 2019. Cited on pages 2, 3, and 4.

[Kim et al., 2018] C. KIM, A. S. BANDEIRA, and M. X. GOEMANS. *Stochastic block model for hypergraphs: Statistical limits and a semidefinite programming approach*. arXiv:1807.02884, 2018. Cited on pages 2 and 4.

[Kumar et al., 2020] T. KUMAR, S. VAIDYANATHAN, H. ANANTHAPADMANABHAN, S. PARTHASARATHY, and B. RAVINDRAN. *Hypergraph clustering by iteratively reweighted modularity maximization*. Applied Network Science, 5 (1), pp. 1–22, 2020. Cited on page 6.

[Lambiotte et al., 2019] R. LAMBIOTTE, M. ROSVALL, and I. SCHOLTES. *From networks to optimal higher-order models of complex systems*. Nature Physics, 15 (4), pp. 313–320, 2019. Cited on page 1.

[Larremore et al., 2014] D. B. LARREMORE, A. CLAUSET, and A. Z. JACOBS. *Efficiently inferring community structure in bipartite networks*. Physical Review E, 90 (1), p. 012805, 2014. Cited on page 4.

[Li and Milenovic, 2017] P. LI and O. MILENKOVIC. *Inhomogeneous hypergraph clustering with applications*. In *Advances in Neural Information Processing Systems*, pp. 2308–2318. 2017. Cited on pages 2 and 4.

[Li and Milenovic, 2018] ———. *Submodular hypergraphs: P-laplacians, cheeger inequalities and spectral clustering*. In *35th International Conference on Machine Learning, ICML 2018*, pp. 4690–4719. 2018. Cited on pages 1, 2, and 4.

[Li et al., 2019] P. LI, G. J. PULEO, and O. MILENKOVIC. *Motif and hypergraph correlation clustering*. IEEE Transactions on Information Theory, 2019. Cited on page 2.

[Li and Solé, 1996] W.-C. W. LI and P. SOLÉ. *Spectra of regular graphs and hypergraphs and orthogonal polynomials*. European Journal of Combinatorics, 17 (5), pp. 461 – 477, 1996. doi:10.1006/eujc.1996.0040. Cited on page 4.

[Liu and Murata, 2010] X. LIU and T. MURATA. *An efficient algorithm for optimizing bipartite modularity in bipartite networks*. Journal of Advanced Computational Intelligence and Intelligent Informatics, 14 (4), pp. 408–415, 2010. Cited on page 5.

[Louis, 2015] A. LOUIS. *Hypergraph markov operators, eigenvalues and approximation algorithms*. In *Proceedings of the Forty-Seventh Annual ACM Symposium on Theory of Computing*, pp. 713–722. 2015. doi:10.1145/2746539.2746555. Cited on page 4.

[Mastrandrea et al., 2015] R. MASTRANDREA, J. FOURNET, and A. BARRAT. *Contact patterns in a high school: a comparison between data collected using wearable sensors, contact diaries and friendship surveys*. PloS one, 10 (9), p. e0136497, 2015. Cited on page 16.

[Milo, 2002] R. MILO. *Network motifs: Simple building blocks of complex networks*. Science, 298 (5594), pp. 824–827, 2002. doi:10.1126/science.298.5594.824. Cited on page 1.

[Murata, 2009a] T. MURATA. *Detecting communities from bipartite networks based on bipartite modularities*. In *2009 International Conference on Computational Science and Engineering*, pp. 50–57. 2009a. Cited on page 5.

[Murata, 2009b] ———. *Modularities for bipartite networks*. In *Proceedings of the 20th ACM Conference on Hypertext and Hypermedia*, pp. 245–250. 2009b. Cited on page 5.

[Nadakuditi and Newman, 2012] R. R. NADAKUDITI and M. E. NEWMAN. *Graph spectra and the detectability of community structure in networks*. Physical Review Letters, 108 (18), p. 188701, 2012. Cited on page 15.

[Neubauer and Obermayer, 2009] N. NEUBAUER and K. OBERMAYER. *Towards community detection in k -partite k -uniform hypergraphs*. In *Proceedings of the 2009 Workshop on Analyzing Networks and Learning with Graphs*, pp. 1–9. 2009. Cited on page 2.

[Newman, 2006] M. E. NEWMAN. *Modularity and community structure in networks*. Proceedings of the National Academy of Sciences, 103 (23), pp. 8577–8582, 2006. Cited on page 21.

[Newman, 2016] ———. *Equivalence between modularity optimization and maximum likelihood methods for community detection*. Physical Review E, 94 (5), p. 052315, 2016. Cited on pages 5, 7, 10, 11, 18, and 21.

[Newman, 2010] M. E. J. NEWMAN. *Networks: An Introduction*. Oxford University Press, 2010. Cited on page 1.

[Newman and Girvan, 2004] M. E. J. NEWMAN and M. GIRVAN. *Finding and evaluating community structure in networks*. Physical Review E, 69, p. 026113, 2004. doi:10.1103/PhysRevE.69.026113. Cited on page 5.

[Nowicki and Snijders, 2001] K. NOWICKI and T. A. B. SNIJDERS. *Estimation and prediction for stochastic blockstructures*. Journal of the American Statistical Association, 96 (455), pp. 1077–1087, 2001. Cited on page 2.

[Peel et al., 2017] L. PEEL, D. B. LARREMORE, and A. CLAUSET. *The ground truth about metadata and community detection in networks*. Science Advances, 3 (5), p. e1602548, 2017. Cited on pages 5 and 20.

[Peixoto, 2014] T. P. PEIXOTO. *Hierarchical block structures and high-resolution model selection in large networks*. Physical Review X, 4 (1), p. 011047, 2014. Cited on page 2.

[Peixoto, 2019] ———. *Bayesian stochastic blockmodeling*. Advances in Network Clustering and Blockmodeling, pp. 289–332, 2019. Cited on pages 7 and 21.

[Porter et al., 2009] M. A. PORTER, J.-P. ONNELA, and P. J. MUCHA. *Communities in networks*. Notices of the AMS, 56 (9), pp. 1082–1097, 2009. Cited on page 2.

[Reichardt and Bornholdt, 2006] J. REICHARDT and S. BORNHOLDT. *Statistical mechanics of community detection*. Physical Review E, 74 (1), p. 016110, 2006. Cited on pages 5 and 11.

[Rodríguez, 2003] J. RODRÍGUEZ. *On the laplacian spectrum and walk-regular hypergraphs*. Linear and Multilinear Algebra, 51 (3), pp. 285–297, 2003. doi:10.1080/0308108031000084374. Cited on page 4.

[Sahasrabuddhe et al., 2020] R. SAHASRABUDDE, L. NEUHÄUSER, and R. LAMBIOTTE. *Modelling non-linear consensus dynamics on hypergraphs*. Journal of Physics: Complexity, 2020. Cited on page 1.

[Schlag et al., 2016] S. SCHLAG, V. HENNE, T. HEUER, H. MEYERHENKE, P. SANDERS, and C. SCHULZ. *k -way hypergraph partitioning via n -level recursive bisection*. In *18th Workshop on Algorithm Engineering and Experiments, (ALENEX 2016)*, pp. 53–67. 2016. Cited on page 4.

[Schwarz, 1978] G. SCHWARZ. *Estimating the dimension of a model*. The Annals of Statistics, 6 (2), pp. 461–464, 1978. Cited on page 17.

[Stehlé et al., 2011] J. STEHLÉ, N. VOIRIN, A. BARRAT, C. CATTUTO, L. ISELLA, J.-F. PINTON, M. QUAGGIOTTO, W. V. DEN BROECK, C. RÉGIS, B. LINA, and P. VANHEMS. *High-resolution measurements of face-to-face contact patterns in a primary school*. PLoS ONE, 6 (8), p. e23176, 2011. doi:10.1371/journal.pone.0023176. Cited on page 16.

[Stewart and Woon, 2021] C. STEWART and J. WOON. *Congressional committee assignments, 103rd to 115th congresses, 1993–2017*. 2021. Cited on page 16.

[Tian et al., 2009] Z. TIAN, T. HWANG, and R. KUANG. *A hypergraph-based learning algorithm for classifying gene expression and arrayCGH data with prior knowledge*. Bioinformatics, 25 (21), pp. 2831–2838, 2009. doi:10.1093/bioinformatics/btp467. Cited on page 2.

[Torres et al., 2020] L. TORRES, A. S. BLEVINS, D. S. BASSETT, and T. ELIASI-RAD. *The why, how, and when of representations for complex systems*. arXiv:2006.02870, 2020. Cited on page 1.

[Traag et al., 2019] V. A. TRAAG, L. WALTMAN, and N. J. VAN ECK. *From Louvain to Leiden: guaranteeing well-connected communities*. Scientific Reports, 9 (1), pp. 1–12, 2019. Cited on page 5.

[Tsourakakis et al., 2017] C. E. TSOURAKAKIS, J. PACHOCKI, and M. MITZENMACHER. *Scalable motif-aware graph clustering*. In *Proceedings of the 26th International Conference on World Wide Web*, pp. 1451–1460. 2017. Cited on page 2.

[Veldt et al., 2020a] N. VELDT, A. R. BENSON, and J. KLEINBERG. *Hypergraph cuts with general splitting functions*. arXiv:2001.02817, 2020a. Cited on pages 3, 9, and 10.

[Veldt et al., 2020b] ———. *Minimizing localized ratio cut objectives in hypergraphs*. In *Proceedings of the 26th ACM SIGKDD International Conference on Knowledge Discovery & Data Mining*, pp. 1708–1718. 2020b. Cited on page 1.

[Veldt et al., 2018] N. VELDT, D. F. GLEICH, and A. WIRTH. *A correlation clustering framework for community detection*. In *Proceedings of the 2018 World Wide Web Conference*, p. 439–448. 2018. doi:10.1145/3178876.3186110. Cited on page 11.

[Veldt et al., 2020c] N. VELDT, A. WIRTH, and D. F. GLEICH. *Parameterized correlation clustering in hypergraphs and bipartite graphs*. In *Proceedings of the 26th ACM SIGKDD International Conference on Knowledge Discovery & Data Mining*, pp. 1868–1876. 2020c. Cited on page 2.

[Weir et al., 2017] W. H. WEIR, S. EMMONS, R. GIBSON, D. TAYLOR, and P. J. MUCHA. *Post-processing partitions to identify domains of modularity optimization*. Algorithms, 10 (3), p. 93, 2017. Cited on page 5.

[Yadati et al., 2019] N. YADATI, M. NIMISHAKAVI, P. YADAV, V. NITIN, A. LOUIS, and P. TALUKDAR. *HyperGCN: A new method for training graph convolutional networks on hypergraphs*. In *Advances in Neural Information Processing Systems*, pp. 1511–1522. 2019. Cited on page 2.

[Yang and Leskovec, 2013] J. YANG and J. LESKOVEC. *Overlapping community detection at scale: a nonnegative matrix factorization approach*. In *Proceedings of the sixth ACM international conference on Web search and data mining*, pp. 587–596. 2013. Cited on page [2](#).

[Yen and Larremore, 2020] T.-C. YEN and D. B. LARREMORE. *Community detection in bipartite networks with stochastic block-models*. arXiv:2001.11818, 2020. Cited on page [4](#).

[Yoshida, 2019] Y. YOSHIDA. *Cheeger Inequalities for Submodular Transformations*, pp. 2582–2601. Society for Industrial and Applied Mathematics, 2019. doi:[10.1137/1.978161975482.160](https://doi.org/10.1137/1.978161975482.160). Cited on page [4](#).

[Zhang and Peixoto, 2020] L. ZHANG and T. P. PEIXOTO. *Statistical inference of assortative community structures*. *Physical Review Research*, 2 (4), p. 043271, 2020. Cited on page [10](#).

[Zhang and Moore, 2014] P. ZHANG and C. MOORE. *Scalable detection of statistically significant communities and hierarchies, using message passing for modularity*. *Proceedings of the National Academy of Sciences*, 111 (51), pp. 18144–18149, 2014. Cited on pages [5](#), [7](#), and [21](#).

[Zhou et al., 2006] D. ZHOU, J. HUANG, and B. SCHÖLKOPF. *Learning with hypergraphs: Clustering, classification, and embedding*. In *Proceedings of the 19th International Conference on Neural Information Processing Systems*, pp. 1601–1608. 2006. Cited on pages [2](#) and [4](#).

SUPPLEMENTARY INFORMATION
Generative Hypergraph Clustering: From Blockmodels to Modularity

A PROOF OF (6)

We prove the identity by direct calculation. We have

$$\begin{aligned}
\sum_{R \in \mathcal{R}} b_R \sigma(\boldsymbol{\theta}_R) \Omega(\mathbf{z}_R) &= \sum_{k=1}^{\bar{k}} \sum_{T \in \mathcal{T}_k} \sigma(\boldsymbol{\theta}_T) \Omega(\mathbf{z}_T) \\
&= \sum_{k=1}^{\bar{k}} \sum_{T \in \mathcal{T}_k} \left(\prod_{i=1}^n \theta_i^{t_i} \right) \Omega(\mathbf{z}_T) \\
&= \sum_{k=1}^{\bar{k}} \sum_{\mathbf{y} \in [\ell]^k} \Omega(\mathbf{y}) \sum_{R \in \mathcal{T}_k} \delta(\mathbf{z}_T, \mathbf{y}) \left(\prod_{i=1}^n \theta_i^{t_i} \right) . \\
&= \sum_{k=1}^{\bar{k}} \sum_{\mathbf{y} \in [\ell]^k} \Omega(\mathbf{y}) \prod_{y \in \mathbf{y}} \sum_{i=1}^n \theta_i \delta(z_i, y) \\
&= \sum_{k=1}^{\bar{k}} \sum_{\mathbf{y} \in [\ell]^k} \Omega(\mathbf{y}) \prod_{y \in \mathbf{y}} \text{vol}(y) ,
\end{aligned}$$

as was to be shown.

B MAXIMUM-LIKELIHOOD ESTIMATION OF Ω

Inserting (6) into the definition of Q yields

$$Q(\mathbf{z}, \Omega, \boldsymbol{\theta}) = \sum_{R \in \mathcal{R}} a_R \log \Omega(\mathbf{z}_R) - \sum_{k=1}^{\bar{k}} \sum_{\mathbf{y} \in [\ell]^k} \Omega(\mathbf{y}) \prod_{y \in \mathbf{y}} \text{vol}(y) .$$

Focusing on the set Y on which Ω takes constant value ω , we write

$$Q(\mathbf{z}, \Omega, \boldsymbol{\theta}) = \sum_{\mathbf{y} \in Y} \left[\delta(\mathbf{z}_R, \mathbf{y}) \sum_{R \in \mathcal{R}} a_R \log \omega - \omega \prod_{y \in \mathbf{y}} \text{vol}(y) \right] + C ,$$

where C captures terms that do not depend on ω . The first-order condition reads

$$0 = \frac{\partial Q}{\partial \omega} = \sum_{\mathbf{y} \in Y} \left[\frac{1}{\omega} \sum_{R \in \mathcal{R}} a_R \delta(\mathbf{z}_R, \mathbf{y}) - \prod_{y \in \mathbf{y}} \text{vol}(y) \right] .$$

Solving for the constant ω yields (8).

C DERIVATION OF (9)

We have

$$\begin{aligned}
Q(\mathbf{z}, \Omega, \boldsymbol{\theta}) &= \sum_{R \in \mathcal{R}} [a_R \log \Omega(\mathbf{z}_R) - b_R \sigma(\boldsymbol{\theta}_R) \Omega(\mathbf{z}_R)] \\
&= \sum_{R \in \mathcal{R}} \sum_{\mathbf{p} \in \mathcal{P}} \delta(\mathbf{p}, \phi(\mathbf{z}_R)) [a_R \log \Omega(\mathbf{z}_R) - b_R \sigma(\boldsymbol{\theta}_R) \Omega(\mathbf{z}_R)] \\
&= \sum_{k=1}^{\bar{k}} \sum_{\mathbf{p} \in \mathcal{P}_k} \left[\sum_{R \in \mathcal{R}_k} a_R \delta(\mathbf{p}, \phi(\mathbf{z}_R)) \log \Omega(\mathbf{p}) - \sum_{\mathbf{y} \in [\bar{\ell}]^k} \delta(\mathbf{p}, \phi(\mathbf{y})) \Omega(\mathbf{p}) \prod_{y \in \mathbf{y}} \text{vol}(y) \right] \\
&= \sum_{k=1}^{\bar{k}} \sum_{\mathbf{p} \in \mathcal{P}_k} [\mathbf{cut}_{\mathbf{p}}(\mathbf{z}) \log \Omega(\mathbf{p}) - \mathbf{vol}_{\mathbf{p}}(\mathbf{z}) \Omega(\mathbf{p})] \\
&= \sum_{\mathbf{p} \in \mathcal{P}} [\mathbf{cut}_{\mathbf{p}}(\mathbf{z}) \log \Omega(\mathbf{p}) - \mathbf{vol}_{\mathbf{p}}(\mathbf{z}) \Omega(\mathbf{p})] ,
\end{aligned}$$

where to obtain the third line we have applied the identity (6).

D DERIVATION OF (10)

The all-or-nothing affinity function for a size- k hyperedge R can be written as

$$\Omega(\mathbf{z}_R) = \omega_{k0} + \delta(\mathbf{z}_R)(\omega_{k1} - \omega_{k0}) = \omega_{k0} + \delta(\mathbf{z}_R)\gamma_k\beta_k, \quad (12)$$

and we also have

$$\log \Omega(\mathbf{z}_R) = \log \omega_{k0} + \delta(\mathbf{z}_R)(\log \omega_{k1} - \log \omega_{k0}) = \log \omega_{k0} + \delta(\mathbf{z}_R)\beta_k. \quad (13)$$

In order to later simplify terms in the modularity objective, first recall that \mathcal{R}_k is the set of unordered k -tuples of nodes, and \mathcal{T}_k is the set of ordered k -tuples. Let $T \subseteq \ell$ indicate that all nodes from an ordered k -tuple $T \in \mathcal{T}_k$ are in cluster ℓ . Then we have

$$\sum_{R \in \mathcal{R}_k} b_R \sigma(\mathbf{d}_R) \delta(\mathbf{z}_R) = \sum_{T \in \mathcal{T}_k} \sigma(\mathbf{d}_T) \delta(\mathbf{z}_T) = \sum_{\ell=1}^{\bar{\ell}} \sum_{T \subseteq \ell} \sigma(\mathbf{d}_T) = \sum_{\ell=1}^{\bar{\ell}} \text{vol}(\ell)^k.$$

Using the fact that $\boldsymbol{\theta}_R = \mathbf{d}_R$, and applying definition of the cut function $\mathbf{cut}_k(\mathbf{z})$, we derive the simplified form of the all-or-nothing modularity objective:

$$\begin{aligned}
Q(\mathbf{z}, \Omega, \boldsymbol{\theta}) &= \sum_{R \in \mathcal{R}} [a_R \log \Omega(\mathbf{z}_R) - b_R \sigma(\boldsymbol{\theta}_R) \Omega(\mathbf{z}_R)] \\
&= \sum_{k=1}^{\bar{k}} \sum_{R \in \mathcal{R}_k} [a_R (\log \omega_{k0} + \delta(\mathbf{z}_R)\beta_k) - b_R \sigma(\mathbf{d}_R)(\omega_{k0} + \delta(\mathbf{z}_R)\gamma_k\beta_k)] \\
&= \sum_{k=1}^{\bar{k}} \sum_{R \in \mathcal{R}_k} [a_R \log \omega_{k0} - b_R \sigma(\mathbf{d}_R)\omega_{k0}] + \sum_{k=1}^{\bar{k}} \beta_k \left[\sum_{R \in \mathcal{R}_k} (a_R \delta(\mathbf{z}_R) - \gamma_k b_R \sigma(\mathbf{d}_R) \delta(\mathbf{z}_R)) \right] \\
&= \sum_{k=1}^{\bar{k}} \sum_{R \in \mathcal{R}_k} [a_R \log \omega_{k0} - b_R \sigma(\mathbf{d}_R)\omega_{k0}] + \sum_{k=1}^{\bar{k}} \beta_k \left[m_k - \mathbf{cut}_k(\mathbf{z}) - \gamma_k \sum_{\ell=1}^{\bar{\ell}} \text{vol}(\ell)^k \right] \\
&= J(\boldsymbol{\omega}) - \sum_{k=1}^{\bar{k}} \beta_k \left[\mathbf{cut}_k(\mathbf{z}) + \gamma_k \sum_{\ell=1}^{\bar{\ell}} \text{vol}(\ell)^k \right]
\end{aligned}$$

where

$$J(\boldsymbol{\omega}) = \left[\sum_{k=1}^{\bar{k}} \beta_k m_k \right] + \left[\sum_{k=1}^{\bar{k}} \sum_{R \in \mathcal{R}_k} (a_R \log \omega_{k0} - b_R \sigma(\mathbf{d}_R)\omega_{k0}) \right].$$

E PROOF OF PROPOSITION 1

Let \mathbf{e}_j be the j th standard basis vector. For each k , let $\mu_k = \sum_{\ell=1}^{\bar{\ell}} \mathbf{vol}(\ell)^k$.

Proposition 1. *Fix \mathbf{p} , and let $r = \|\mathbf{p}\|_0$ be the number of nonzero elements of \mathbf{p} . Then,*

$$U_{\mathbf{p}} = \mu_{p_r} U_{\mathbf{p}-p_r \mathbf{e}_r} - \sum_{j=1}^{r-1} U_{\mathbf{p}+p_r(\mathbf{e}_j - \mathbf{e}_r)} .$$

Proof. For notational compactness, let $v_{\ell} = \mathbf{vol}(\ell)$. Let $r = \|\mathbf{p}\|_0$ be the number of nonzero elements in \mathbf{p} . By definition, we have

$$U_{\mathbf{p}} = \binom{k}{\mathbf{p}}^{-1} \prod_{j=1}^k |\{h : p_h = j\}|! \sum_{\mathbf{y} \in [\ell]^k} \delta(\mathbf{p}, \phi(\mathbf{y})) \prod_{y \in \mathbf{y}} v_y .$$

For a given label vector \mathbf{y} such that $\phi(\mathbf{y}) = \mathbf{p}$, there are $\binom{k}{\mathbf{p}} \prod_{j=1}^k (|\{h : p_h = j\}|!)^{-1}$ ways to permute the labels of \mathbf{y} . The number $U_{\mathbf{p}}$ thus has exactly one term of the form $\prod_{y \in \mathbf{y}} v_y$ for each equivalence class of label vectors under permutation. We thus obtain the simplification

$$U_{\mathbf{p}} = \sum_{t_1 \neq \dots \neq t_r} \prod_{j=1}^r v_{t_j}^{p_j} .$$

Peeling off the r th term in this product gives

$$\begin{aligned} U_{\mathbf{p}} &= \sum_{t_1 \neq \dots \neq t_{r-1}} \prod_{j=1}^{r-1} v_{t_j}^{p_j} \sum_{\ell \notin \{t_1, \dots, t_{r-1}\}} v_{\ell}^{p_r} \\ &= \sum_{t_1 \neq \dots \neq t_{r-1}} \prod_{j=1}^{r-1} v_{t_j}^{p_j} \left[\sum_{\ell=1}^{\bar{\ell}} v_{\ell}^{p_r} - \sum_{j'=1}^{r-1} v_{t_j'}^{p_r} \right] . \end{aligned} \quad (14)$$

We first recognize

$$\sum_{t_1 \neq \dots \neq t_{r-1}} \prod_{j=1}^{r-1} v_{t_j}^{p_j} = U_{\mathbf{p}-p_r \mathbf{e}_r} \quad \text{and} \quad \sum_{\ell=1}^{\bar{\ell}} v_{\ell}^{p_r} = \mu_{p_r} .$$

We next observe that

$$\sum_{t_1 \neq \dots \neq t_{r-1}} \prod_{j=1}^{r-1} v_{t_j}^{p_j} \sum_{j'=1}^{r-1} v_{t_j'}^{p_j} = \sum_{j=1}^{r-1} U_{\mathbf{p}+p_r(\mathbf{e}_j - \mathbf{e}_r)} .$$

Inserting these identities into (14) completes the proof. \square

We note that Proposition 1 also gives an efficient recursive update for the numbers $U_{\mathbf{p}}$ when moving nodes between clusters. Let \mathbf{z} and \mathbf{z}' be distinct label vectors, and let $\{\mu_k\}$ and $\{\mu'_k\}$ be the moments of volumes evaluated with respect to \mathbf{z} and \mathbf{z}' respectively. Then, applying Proposition 1 twice yields the update $\Delta U_{\mathbf{p}} = U'_{\mathbf{p}} - U_{\mathbf{p}}$:

$$\Delta U_{\mathbf{p}} = (\Delta \mu_{p_r}) U_{\mathbf{p}-p_r \mathbf{e}_r} + \mu_{p_r} (\Delta U_{\mathbf{p}-p_r \mathbf{e}_r}) + (\Delta \mu_{p_r}) (\Delta U_{\mathbf{p}-p_r \mathbf{e}_r}) - \sum_{j=1}^{r-1} \Delta U_{\mathbf{p}+p_r(\mathbf{e}_j - \mathbf{e}_r)} .$$

We can thus use Proposition 1 to compute the set of numbers $\{U_{\mathbf{p}}\}$ once “from scratch,” and then efficiently update these numbers as the label vector changes in the course of optimization.

Algorithm 3: AllOrNothingHMML(H, β, γ)

Data: Hypergraph H , parameter vectors β and γ

Result: Updated label vector \mathbf{z}

```

 $\mathbf{z}' \leftarrow \mathbf{z} \leftarrow [n]$  // assign each cluster to singleton
do
   $\mathbf{z} \leftarrow \mathbf{z}'$ 
   $\bar{H}, \bar{\mathbf{s}} \leftarrow \text{Collapse}(H, \mathbf{z})$ 
   $\bar{\mathbf{z}}' \leftarrow \text{AONLouvainStep}(\bar{H}, \bar{\mathbf{s}}, \beta, \gamma)$ 
   $\mathbf{z}' \leftarrow \text{Expand}(H, \bar{\mathbf{z}}')$ 
while  $\mathbf{z} \neq \mathbf{z}'$ 
return  $\mathbf{z}$ 

```

**F ALL-OR-NOTHING HYPERGRAPH
MAXIMUM-LIKELIHOOD LOUVAIN**

In Section 5.1, we gave pseudocode for Hypergraph Maximum-Likelihood Louvain (HMML) for general symmetric affinity functions Ω (Algorithms 1 and 2). For the special case of the All-Or-Nothing affinity function, it is possible to obtain a considerably faster Louvain algorithm. In particular, it is possible to follow the “supernode” strategy of classical dyadic Louvain, enabling to compute on data structures much simpler than the original adjacency hyperarray. Algorithm 3 describes the outer loop of AON HMML. The overall structure is much the same as in Algorithm 2. In order to realize the efficiencies of the special AON structure, we perform the main Louvain step on a reduced hypergraph \bar{H} , with the functions $\text{Collapse}(H, \mathbf{z})$ and $\text{Expand}(H, \bar{\mathbf{z}})$ translating between full and reduced representations. In constructing the reduced representation \bar{H} , it is necessary only to store only the collapsed hypergraph alongside a vector $\bar{\mathbf{s}}$ of original sizes of each edge. The degree \bar{d}_ℓ of each collapsed node ℓ is simply the sum of degrees of nodes in the corresponding cluster ℓ .

The Louvain step itself is given by Algorithm 4. At each stage, we examine a collapsed node i and compute the change in objective associated with changing $\bar{\mathbf{z}}$ to $\bar{\mathbf{z}}^{i \mapsto A}$, where

$$\bar{\mathbf{z}}_j^{i \mapsto A} = \begin{cases} A & i = j \\ \bar{\mathbf{z}}_j & \text{otherwise} \end{cases},$$

is the collapsed label vector obtained by setting $z_i \mapsto A$ while leaving other entries unchanged. This calculation is contained within the subroutine ΔQ_{AON} (Algorithm 5). Notably, evaluation of ΔQ_{AON} is much faster than the evaluation of ΔQ in the general symmetric case Algorithm 1. Local changes in the volume term of (10) requires only updating sums of powers of cluster volumes, scaled by the resolution parameters β and γ . Updates to the cut term of (10) requires summing over the changes in cut status of each hyperedge adjacent to the node i to be updated. In the AON setting, there are only two possible statuses—cut and uncut. Checking whether an edge is cut is much easier than computing an exact partition vector for a hyperedge before and after a potential move. This step is therefore much faster in practice than computing cut changes for the symmetric objective.

Algorithm 4: AONLouvainStep(\bar{H} , \bar{s} , β , γ_ℓ)

Data: Collapsed hypergraph $\bar{H} = (\bar{V}, \bar{E})$, edge size vector \bar{s} , parameter vectors β and γ

Result: Label vector \bar{z} on \bar{V}

```

 $\bar{z} \leftarrow [\bar{n}]$                                 //  $\bar{n}$  is the number of nodes in  $\bar{H}$ 
improving  $\leftarrow$  true
while improving do
  improving  $\leftarrow$  false
  for  $i \in \bar{V}$  do
     $\mathcal{E}_i \leftarrow \{e \in \bar{E} \mid i \in e\}$           // hyperedges incident on node  $i$ 
     $\mathcal{A}_i \leftarrow \{\ell \mid \exists j \in \mathcal{E}_i : z_j = \ell\}$  // clusters adjacent to node  $i$ 
    // maximum  $\Delta$  and maximizer  $A$  of the change in  $Q$  from moving
    // node  $i$  to cluster  $A' \in \mathcal{A}_i$ 
     $(\Delta, A) \leftarrow \text{argmax}_{A' \in \mathcal{A}_i} \Delta Q_{\text{AON}}(\bar{H}, \bar{z}, \bar{s}, A', i, \mathcal{E}_i, \beta, \gamma)$ 
    if  $\Delta > 0$  then
      |  $\bar{z}_i \leftarrow A$ , improving  $\leftarrow$  true
    end
  end
end

```

Algorithm 5: $\Delta Q_{\text{AON}}(\bar{H}, \bar{z}, \bar{s}, A, i, \mathcal{E}_i, \beta, \gamma)$

Data: Collapsed hypergraph $\bar{H} = (\bar{V}, \bar{E})$, current clustering \bar{z} , edge size vector \bar{s} , proposed new cluster A , node to move i , edge set incident to i \mathcal{E}_i , parameter vectors β and γ

Result: Change in modularity associated with moving node i to new cluster A

```

 $v_A \leftarrow \text{vol}(A)$ ,  $v_i \leftarrow \text{vol}(\bar{z}[i])$ 
 $\Delta v = \sum_{k=1}^{\bar{k}} \beta_k \gamma_k [v_i^k - (v_i - \bar{d}_i)^k + v_A^k - (v_A + \bar{d}_i)^k]$ 
 $\Delta c = \sum_{e \in \mathcal{E}_i} \beta_{\bar{s}_i} [\delta(\bar{z}_e^{i \rightarrow A}) - \delta(\bar{z}_e)]$ 
return  $\Delta c + \Delta v$ 

```
